Universitatea
Transilvania
din Brașov

INTERDISCIPLINARY DOCTORAL SCHOOL

Faculty of Silviculture and Forest Engineering

Eng. Andrei BUZATU

MONITORING AND ASSESSMENT OF THE PHYTOSANITARY STATUS OF FORESTS USING SOME REMOTE SENSING TECHNIQUES

ABSTRACT

Scientific coordinator

CS I. PhD. Eng. Nicolae Ovidiu BADEA

BRAȘOV, 2023

CONTENTS

1. INTRODUCTION

Defoliating insects causing the most significant damage in deciduous forests include *Lymantria dispar* (Linnaeus, 1758), *Tortrix viridana* (Linnaeus, 1758), and various species of Geometridae (*Operophtera brumata* (Linnaeus, 1758), *Erannis defoliaria* (Clerck, 1759), *Erannis aurantiaria* (Hübner, 1796-1799), *Erannis marginaria* (Fabricius, 1777), *Erannis leucophaearia* (Schiffermüller), etc.), which frequently develop large-scale outbreaks in oak forests. In last years, also in oak forests, as a result of climate change and intensified intercontinental trade, significant damage has been reported, caused by the invasive species *Corythucha arcuata* (Hemiptera, Tingidae, Say, 1832), of North American origin, manifested through discoloration of the tree foliage. In coniferous forests, especially spruce forests, the most important damage can be caused by the defoliating insect *Lymantria monacha*, whereas for fir forests, *Choristoneura murinana* (Hübner, 1799) and *Zeiraphera (Semasia) rufimitrana* (Herrich-Schäffer, 1851) are responsible, but with very rare outbreaks.

Until now, in Romania, monitoring the actions of harmful biotic and abiotic factors has been conducted exclusively from the ground, through direct observations.

Considering the technological advancements and the existing concerns in other countries, it is imperative for our country to develop a forest ecosystem surveillance system based on remote sensing techniques using satellite imagery or aerial images captured through Unmanned Aerial Vehicles (UAVs), commonly known as drones. These UAVs will be equipped with various specialized sensors for image capture. Both satellite and drone-captured images can be subsequently utilized for analysis and interpretation. The sensors on board of drones and satellites capture aerial digital images based on electromagnetic radiation emitted by ground features from an external source, such as the sun. These images can be acquired in various spectral bands, including the visible spectrum (RGB), near-infrared (NIR), infrared (IR), thermal, hyperspectral, among others (Vorovencii, 2015).

These technologies are based on the fact that any object receiving energy absorbs from the sun, transmits, and reflects electromagnetic radiation with different wavelengths back into the atmosphere, generating a particular model of the reflectance signal (C. D. Rullan-Silva et al., 2013). This specific signal, known as spectral signature, allows the detection, identification, and classification of various forms of tree damage, such as defoliation, discoloration, wind or snowbreak, drying, etc., caused by negative actions of biotic or abiotic factors (Ciesla et al., 2008, C. D. Rullan-Silva et al., 2013).

Applying remote sensing techniques using satellite and aerial imagery allows mapping and understanding of the spatial and temporal distribution of damage intensity caused by various biotic and abiotic factors (Hall et al., 2016).

Mapping vegetation or insect attacks involves using classification algorithms (unsupervised, supervised) to obtain thematic maps. In recent times, a relatively new classification technique based on regression tree methodology has been utilized, a non-parametric method with similar or even better accuracy than specific supervised or unsupervised classifications (Vorovencii, 2015).

Internationally, concerns regarding the use of aerial images for forest protection have existed for more than 75 years (Hall et al., 2016), provide a brief history of remote sensing techniques, mentioning several studies. The first studies were conducted as early as 1946 in North America. Black-and-white infrared images captured from planes or helicopters depicted defoliation based on grayscale nuances. In this representation, darker shades represented healthy trees (Spurr, 1946). In 1951, comparisons were made between panchromatic, infrared, and natural aerial images to evaluate damages caused by *Dendroctonus brevicomis* (LeConte, 1876) (Wear and Bongberg, 1951). In 1978, photographs in visible and infrared domains were used to assess defoliation caused by *Lymantria dispar* (Talerico et al., 1978).

The use of satellite images in forest protection activities was studied from the 1970s, with the advent of the first satellite programs (Landsat 1 - 1972, SPOT 1 - 1986), especially in the United States and Canada. In 1974, Landsat 1 satellite images were used to map damages caused by the defoliator *Lambdina fiscellaria* (Guenée, 1857) (Beaubien et al., 1974) (Hall et al., 2016).

The use of drones for capturing aerial digital images and their application in forest health monitoring is relatively recent, with potential widespread use in the future. In 2014, in Scotland, a thermal imaging sensor mounted on a drone was used to monitor damages resulting in increased crown temperatures in stands of *Pinus sylvestris* (Linnaeus 1753) and *Pinus contorta* (Douglas ex Loudon 1838) affected by *Dothistroma pini* (Hulbary, 1941). A fixed-wing drone, Qpod (QuestUAV Ltd., United Kingdom), equipped with a TIR PI450 camera (Optris GmbH, Germany), and a digital VNIR DMC-LX5 camera (Panasonic Ltd., Japan) were used for data collection. Through visual evaluations on the ground, the proportion of crown area affected by *Dothistroma pini* was estimated. Based on thermal images, temperatures at the crown level were determined by averaging at least six central pixels of each crown. These values were then compared with ground-measured infection levels, resulting in a moderately positive correlation ($R = 0.527$, $p = 0.001$) between temperature and damage intensity progression (Smigaj et al., 2014).

Research has also been conducted in Finland to explore the possibility of using photogrammetry based on hyperspectral aerial images captured by UAVs to map discolorations caused by *Ips typographus* (Linnaeus, 1758) in tree crowns in an urban forest in the southern part of the country. An octocopter equipped with a Fabry-Perot Interferometer (FPI) hyperspectral camera capturing data in 22 bands with wavelengths ranging from 500 to 900 nm (VNIR) was used. RGB images from a separate flight mission were also taken with a Samsung NX1000 camera (Samsung Ltd., South Korea). Using the collected aerial images, digital terrain models were generated, and for each tree, crown models were created. Spectral features were extracted, allowing for classification into three classes (healthy, infested, dead trees), with an overall accuracy of 76%. For two-class classification (healthy and dead trees), the achieved overall accuracy was 90%. Isolated trees were detected with a precision of 74.7% (Näsi et al., 2015).

In the summer of 2013, research was conducted using near-infrared (NIR) aerial images captured by sensors installed on UAVs. The studies were located in northwest Germany (Northrhine Westfalia), in two forest stands infested with *Agrilus biguttatus* (Fabricius, 1777). Thematic maps were created based on the infestation levels using a quadcopter MD4-200 (Microdrones GmbH, Germany) equipped with a VIS-RGB IXUS 100 camera (Canon Inc., Japan), modified to record near-infrared spectrum data. Collected aerial images were assembled using PhotoScan Professional Edition 0.9.0 (Agisoft LLC, Russia) and georeferenced in ArcGIS v. 10.2 (ESRI, USA) using ground control points and distinctive objects on the terrain. Image classification was based on NDVI, resulting in five vegetation cover classes (healthy branches, infested branches, dead branches, other vegetation, and canopy gaps), with a high overall accuracy of 0.81 (very good) for the 0.85 ha forest stand and 0.77 (good) for the 2.05 ha forest stand (Lehmann et al., 2015).

Starting in 2017, experimental flights were conducted using various types of drones (fixed-wing, quadcopter) equipped with both visible (RGB) and thermal imaging sensors. The flights aimed to study the possibility of using aerial images for evaluating damages caused by defoliating insects or windfall. In the summer of 2017, flights were conducted to capture defoliation caused by *Tortrix viridana* using a fixed-wing drone eBee SenseFly equipped with both RGB and thermal (ThermoMap) sensors. The flights were divided into three stages: before aerial treatments, after severe infestations, and after re-foliation. For capturing thermal images, multiple flight altitudes were chosen: 100 m, 120 m, 130 m, and 150 m. Due to adverse weather conditions (low temperatures, strong winds) during larval feeding and high mortality resulting from aerial treatments (98.2% efficacy), the defoliation levels were low (almost imperceptible) (5-10%) and evenly distributed. As a result, ground observations of defoliation and information from visible (RGB) aerial images showed a low level of damage. The analysis of damage characteristics and thermal images taken with the drone at different altitudes did not reveal a clear correlation between defoliation and crown temperature. Given the high efficacy of the applied treatments and the low levels of defoliation, the differences in grayscale on orthophotoplans were not related to damages. Consequently, no conclusive results could be drawn regarding the use of thermal sensors for assessing defoliation caused by insects (Buzatu, 2020).

In the autumn of 2018, a quadcopter type drone, 3DR Solo, equipped with a visible imaging sensor (GoPro Hero 3), was used to observe discolorations on oak trees caused by *Corythucha arcuata*. The communication interface between the drone and the user (tablet) was facilitated by the specialized Solex program. The flight altitude varied in increments of 10 m, ranging from 50 m to 120 m. On the

ground, 30 points were marked with the help of a GPS device, Trimble Juno SB, to determine various tree species (pedunculate oak, linden, ash, pear, etc.) present in the forest, along with different infestation levels of *Corythucha arcuata*. From the set of collected aerial images, a representative image taken at an altitude of 100 m was selected. It was georeferenced based on known ground control points using the ArcGIS program. Subsequently, the image was subjected to classification processes, revealing differences between tree species and different levels of discoloration caused by Corythucha arcuata on the crowns of oak trees (Buzatu, 2020).

2. AIM AND OBJECTIVES

The research carried out **aimed** to use of remote sensing methods for monitoring, assessing and classifying different forms of tree damage, caused by different harmful biotic agents, through the comparative analysis of information provided by digital images (satellite/aerial) with those obtained from field.

The overall objective of the research is to determine the possibilities of using satellite and drone-captured images for the detection, monitoring, and assessment of defoliation caused by *Lymantria dispar* and discolorations caused by *Corythucha arcuata* in oak forest ecosystems.

To achieve the general objective, several **specific objectives** were established:

- Determine the quantitative and qualitative characteristics of the populations of both insect species in the experimental areas and ground-based assessment of damages caused by these insect species.

- Assess damages caused by the two species using satellite images through biophysical and vegetation indices calculated from visible (RGB) and near-infrared (NIR) spectral domains.

- Assess damages caused by the two species using images captured by drones through vegetation indices calculated from visible (RGB) and near-infrared (NIR) spectral domains.

- Comparative analysis of the results obtained from the assessments of damages caused by the two species derived from digital images (satellite/aerial) with those obtained from ground-based observations.

3. MATERIAL AND METODOLOGY

3.1. LOCATION

For both defoliations caused by *Lymantria dispar* and discolorations caused by *Corythucha arcuata*, which result in damages to the oak forest ecosystems, the studies were focused on a forest stand located in the Oltenia region, where *Lymantria dispar* defoliator experienced a gradient outbreak during the period 2018-2020 and *Corythucha arcuata* caused damages in the year 2021 (figure 1). The forest stand is situated within the jurisdiction of the Dolj Forest, Ciuturica Forest Stand (44°15'N - 23°31'E) (figure 2), within the I Criva Forest Management Unit, Craiova Forest District. The forest stand is located in a plain area at an average elevation of 165 meters, covering an approximate area of 310 hectares. It is predominantly composed of turkey oak (Quercus cerris) and hungarian oak (Quercus frainetto) species, with an average age of 65 years and varying density ranging from 0.5 to 0.9.

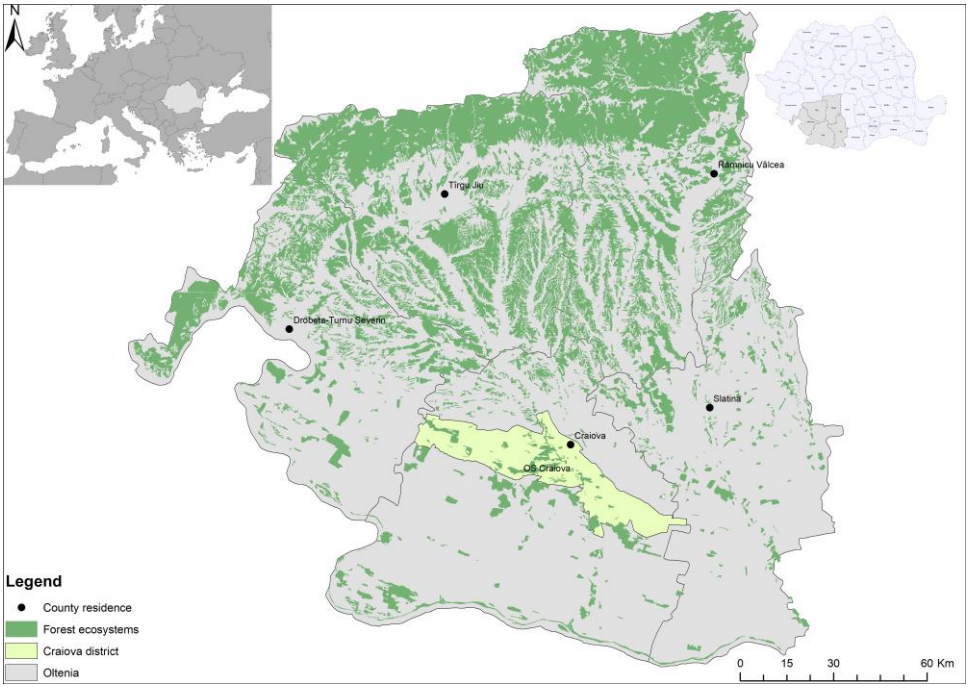

Figure 1. Location

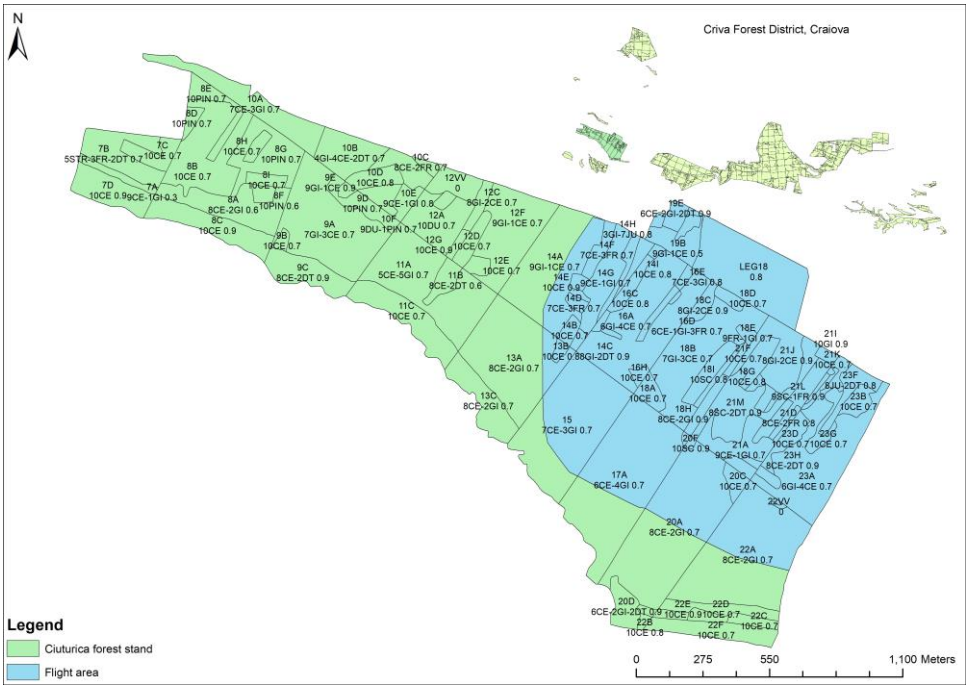

Figure 2. Ciuturica forest stand

3.2. METHODOLOGY

3.2.1. Monitoring insect activity and assessing damages on field

Monitoring and assessing the phytosanitary condition of forests entails a continuous surveillance of their status. Surveillance is an operational component within the framework of integrated pest management, through which the trends in evolution over time, the areas of distribution, and the damages caused by pests are established. The surveillance methods are determined based on the size of the forest area, the biotic or abiotic agents being monitored, and the tree species affected. (Berryman, 1986)

The damages caused by the two insect species in the Ciuturica forest stand, in the years 2020 and 2021, although of different types (defoliations – *Lymantria dispar*, discolorations – *Corythucha arcuata*), occur at the level of the canopy.

Defoliation refers to the loss (total or partial consumption) of leaves or needles from the canopy of a tree, compared to another tree whose foliage is intact (reference tree). (Berryman, 1986).

The defoliations caused by *Lymantria dispar* were estimated through visual assessment of the canopy of the trees within the sample areas of one hectare each, expressed in whole values, in increments of five percent (5, 10, 15 ... %). A reference tree of the same species with complete foliage was used as a comparison. The recorded percentage data were categorized into five degrees of defoliation: very weak 1-10%, weak 11-25%, medium 26-50%, strong 51-75%, and very strong >75%.

The discolorations caused by the invasive insect *Corythucha arcuata*, were estimated through visual assessment of the proportion of leaf mass deviating from the normal color. The recorded data were then divided using the same assessment scale as used for the defoliations caused by *Lymantria dispar*.

To establish the quantitative and qualitative characteristics of the populations of the two insect species and to conduct field evaluations of the damages caused by them, a rectangular grid network of 70 sample plots was established. These sample plots had dimensions of one hectare each and were in a square shape with a side length of 100 meters. The creation of these plots was facilitated using GIS software programs such as ArcGIS (ESRI, USA) (using the Create Fishnet function within the Data Management Tools - Feature class module) and AutoCAD (AutoDesk, USA). The corners of these sample plots were marked in the field with the assistance of a Trimble Juno SB GPS device (Trimble, USA). Around each corner of these sample plots, circular sampling areas with a radius of 12.62 meters (500 m²) were established. Within these circular areas, observations were conducted to assess both the quantitative (density, spatial distribution) and qualitative (fecundity, parasitism, sterility, sex ratio) characteristics of the populations of the two insect species. Furthermore, the level of infestations and the extent of damages caused by these species were determined for the two years under study (figure 3).

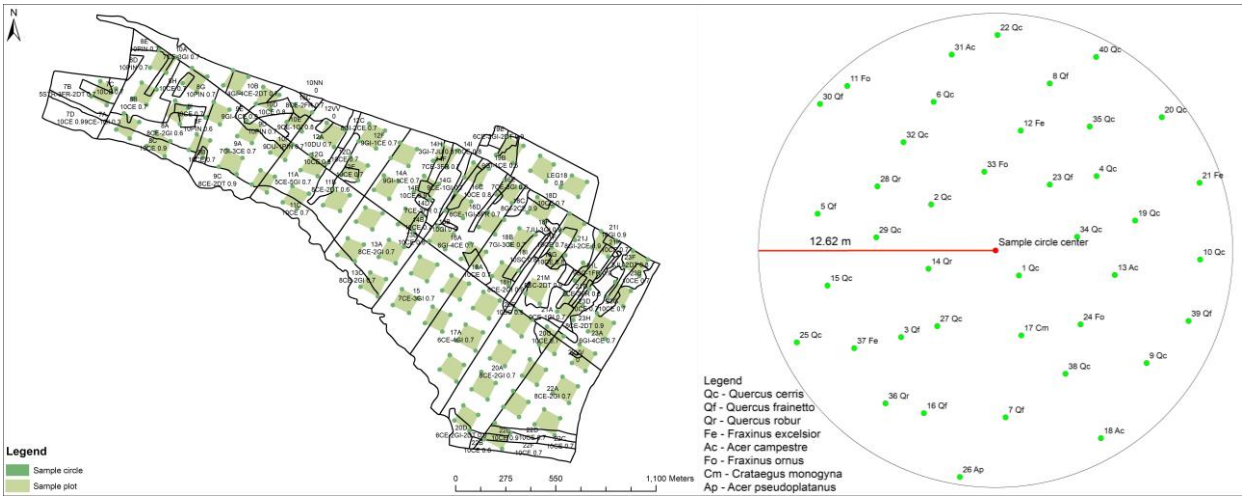

Figure 3. The rectangular network of sample areas located in the Ciuturica forest stand, with detail on the sample circle where observations were made

The data recorded within the sample circles regarding population density, the level of defoliation caused by *Lymantria dispar*, and the discolorations caused by *Corythucha arcuata* were utilized to create thematic maps for the two years of damage (2020 and 2021) using the ArcGIS software. This was achieved by employing the specific interpolation function known as "Inverse Distance Weighted" (IDW), which is part of the "Spatial Analyst Tools – Interpolation – IDW" toolkit. This process facilitated the determination of the affected areas with varying degrees of damage across the Ciuturica forest stand.

To compare the information from the thematic maps based on ground observations with the information provided by digital images, Sentinel-2 satellite images were acquired from the Copernicus platform (European Space Agency - ESA) for the Ciuturica forest stand area for the years 2020 and 2021. These images were obtained during the third decade of July, after the larval feeding process ceased and before the defoliated trees began to re-foliate (figure 4).

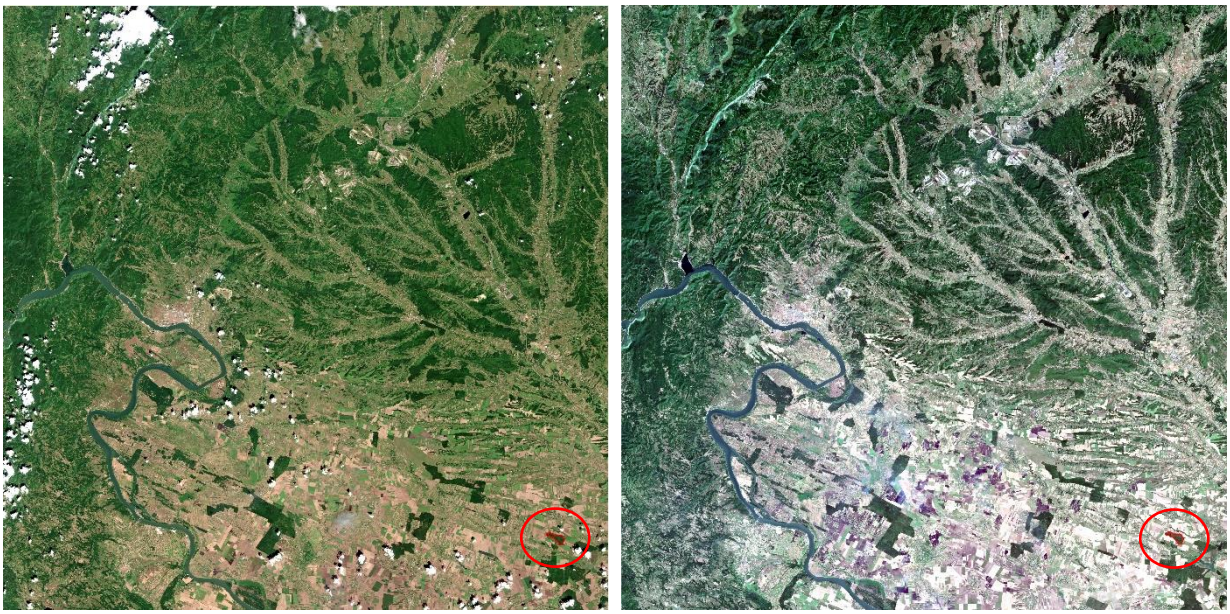

22.07.2020 27.07.2021

Figure 4. Sentinel-2 satellite images from the studied area during the two years of damage, highlighting the Ciuturica forest stand

For easier processing, considering that the forest stand covers a relatively small area of approximately 310 hectares, while a raw satellite image covers about 1,205,000 hectares, the studied forest stand was extracted from the raw satellite image. This was achieved using the "Extract by Mask" function (Spatial Analyst Tools, Extraction) in ArcGIS, using the polygon representing the outline of the forest stand as the masking feature ("mask") (figure 5).

22.07.2020 27.07.2021

Figure 5. Sentinel 2 satellite images for Ciuturica forest stand

The aerial digital images captured using a drone were obtained in the summer of 2020 for the eastern part of the Ciuturica forest stand (approximately 100 hectares), following the completion of larval feeding and pupation. These images were acquired through flights conducted using a fixed-wing drone, the *eBee Plus* (senseFLY SA, Switzerland), equipped with a visible spectrum camera, the senseFly S.O.D.A. (senseFLY SA, Switzerland). Similarly, during the summer of 2021, in the same location and over the same area, flights were carried out using the same type of drone, equipped with a multispectral imaging sensor, the multiSPEC 4C (senseFLY SA, Switzerland).

The *eBee Plus* drone is a lightweight fixed-wing type (1.1 kg) (Figure 6a, b) that can be equipped with RGB, multispectral, and thermal imaging sensors. Flight planning and control are achieved using the *eMotion 3* software (senseFLY SA, Switzerland). The connection is established through radio waves, providing real-time information about the drone's position, battery autonomy, flight time, distance, connection quality, wind speed and direction, ground speed, and flight altitude (Figure 6c) (source: www.sensefly.com).

a b c

Figure 6. The fixed-wing drone eBee (a, b) and a close-up of the eMotion software (c)

The *senseFly S.O.D.A*., visible spectrum imaging sensor, has a resolution of 20 megapixels and enables image capture in the spectral bands of red (660 nm), green (520 nm) and blue (450 nm), with a ground resolution of 2.3 cm/pixel from an altitude of 100 meters.

The *multiSPEC 4C* multispectral imaging sensor allows for image capture in the spectral bands of green (550 nm), red (660 nm), red edge (735 nm), and near-infrared (NIR, 790 nm), with a ground resolution of 10 cm/pixel from an altitude of 100 meters.

The flight missions were conducted based on a predefined flight plan at an altitude of 305 meters (2020) and 265 meters (2021), with an image overlap of 80 meters both along the flight path and laterally.

The aerial digital images captured by the drone were processed using the specialized software *Pix4D* (senseFLY SA, Switzerland), resulting in the overall aerial digital image of the forest stand (figure 7).

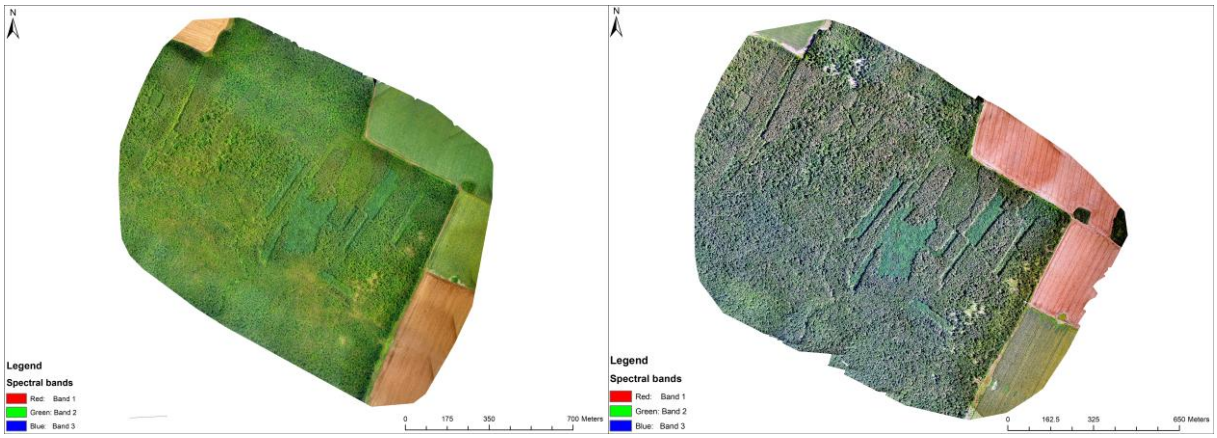

a b

Figure 7. Images captured with the help of the drone for the eastern part of the Ciuturica forest stand, in the years 2020 (a) and 2021 (b).

Considering the higher resolution of the images obtained with the drone compared to satellite images, in the year 2020, when the level of defoliation was higher, ground assessments were conducted for 70

individual trees with varying degrees of defoliation within the drone's flight polygon, aiming for a more detailed analysis of the additional information provided by the drone-captured images (figure 8).

Figure 8. The individual tree locations, with a focus on crown details

3.2.2. Damages monitoring and assessment using digital satellite and aerial imagery

For the present research, composite color images from the visible domain (RGB) and multispectral images based on the near-infrared (NIR) band were utilized.

The images from the visible domain were employed for identifying, monitoring, and assessing damages caused by foliar-feeding insects, resulting in defoliation (*Lymantria dispar*) or discoloration (*Corythucha arcuata*), by determining various vegetation indices.

Considering that vegetation possesses a unique spectral signature in the near-infrared domain, multispectral images were employed to highlight various degrees of damage. Vegetation reflects poorly in both the blue and red regions due to the absorption of radiation by chlorophyll for photosynthesis. It exhibits a peak in the region responsible for the vegetation's color (green), while in the near-infrared zone, reflectance is significantly higher than in the visible bands due to the cellular structure of leaves. Consequently, the aerial image is depicted in varying shades of red, depending on the health condition of the trees. (Vorovencii, 2015)

Based on this strong contrast in vegetation's behavior regarding electromagnetic energy absorption and reflection, a series of biophysical indices (LAI, FAPAR, FVC, CAB, CWC) (table 1) and a multitude of vegetation indices have been developed (G%, GLI, RGBVI, NDVI, EVI, etc.) (table 2).

The *biophysical indices* are obtained through calculation algorithms that mainly involve generating databases with vegetation characteristics and spectral reflectances from the upper part of the canopy, based on various satellite images (Sentinel 2, Landsat 8, MERIS, SPOT). (Weiss et al., 2020).

Table no. 1. Biophysical indices for multispectral digital images

Biophysical indices	Definition	Reference
Leaf Area Index	LAI – is defined as half of the total area of active photosynthetic elements of vegetation (leaves) per unit of horizontal ground surface area.	(Weiss et al., 2020)
Fraction of Absorbed Photosynthetically Active Radiation index	FAPAR – corresponds to the fraction of photosynthetic radiation absorbed by the canopy and depends on the structure of the forest, optical properties of vegetation, and lighting conditions.	(Weiss et al., 2020)
Fractional Vegetation Cover	FVC – corresponds to the fraction of displacement for the nadir direction and is used to distinguish between vegetation and soil in energy balance processes, including temperature and evapotranspiration, and it is not dependent on lighting conditions as compared to FAPAR.	(Weiss et al., 2020)
Chlorophyll a and b	Cab - represents the total amount of chlorophyll in a leaf	(Ali et al.,

	per unit of area and is used as an indicator of stress due to nitrogen deficiency and photosynthetic efficiency.	2020)
Canopy Water Content	CWC – estimates the amount of water stored in leaves per unit of area.	(Cernicharo et al., 2013)

The biophysical indices were automatically obtained using the SNAP software (ESA Sentinel Application Platform v8.0), which, based on vegetation characteristics and spectral reflectance, directly facilitates the calculation of these index values.

Vegetation indices mathematically represent a number generated by specific combinations of bands from digital images, and they are linked to the amount of vegetation within a pixel. It is noted in the literature that these vegetation indices are generally based on empirical evidence rather than biological, physical, or chemical foundations. (Vorovencii, 2015)

Table no. 2. Vegetation indices for near infrared (NIR) and visible (RGB) digital imagery

Vegetation indices	Calculation algorithm	Reference
NIR		
Normalized Difference Vegetation Index	NDVI=(NIR-R)/(NIR+R)	(Rouse et al., 1974)
Soil-Adjusted Vegetation Index	SAVI=((NIR-R)/(NIR+R+0.5))X1.5	(Huete, 1988)
Modified Soil-Adjusted Vegetation Index 2	MSAVI2=1/2(2(NIR+1)-$\sqrt{((2NIR+1)^2-8(NIR-R))}$	(Qi at al., 1994)
Difference Vegetation Index	DVI=NIR-R	(Richardson et al., 1977)
Ratio Vegetation Index	RVI=NIR/R	(Richardson et al., 1977; Vorovencii, 2015)
Perpendicular Vegetation Index	PVI= (NIR-a*XR-b*)/$\sqrt{(1+a^{2*})}$	(Richardson et al., 1977; Vorovencii, 2015)
Infrared Percentage Vegetation Index	IPVI=NIR/(NIR+R)	(Crippen, 1990)
Weighted Difference Vegetation Index	WDVI=NIR-R	(Clevers, 1991)
Transformed Normalized Difference Vegetation Index	TNDVI=$\sqrt{\frac{NIR-R}{NIR+R}+0,5}$	(Tucker, 1979; Senseman et. al., 1996
Green Normalized Difference Vegetation Index	GNDVI=(NIR-G)/(NIR+G)	(Gitelson et al., 1996)
Atmospherically Resistant Vegetation Index	ARVI=(NIR-rb**)/(NIR+rb**)	(Kaufman și Tanre, 1992)
Normalized Difference Index 45	NDI45=(Re_{705}-R_{665})/(Re_{705}+R_{665})***	(Delegido et al., 2011b)
Inverted Red-Edge Chlorophyll Index	IRECI=(Re_{783}-R_{665})/(Re_{705}/Re_{740})***	(Frampton et al., 2013)
Pigment Specific Simple Ratio	PSSRa=Re_{783}/R_{665}***	(Blackburn, 1998)
Normalised Difference Red Edge	NDRE=(NIR-Re_{705})/(NIR+Re_{705})	(Gitelson et al., 1994)
Inverse Ratio Vegetation Index	IRVI=R_{665}/NIR	(Junior et al., 2016)
Green Ratio Vegetation Index	GRVI=NIR/G	(Sripada et al., 2006)
Vogelmann Red Edge Index	VREI=NIR/Re_{705}***	(Vogelmann et al., 1993)
RGB		
Modified Photochemical Reflectance Index	MPRI=(G-R)/(G+R)	(Yang et al., 2008)
Visible Atmospherically Resistant Index	VARI=(G-R)/(G+R-B)	(Gitelson et al. 2002)

Green Percentage Index	G%=G/(R+G+B)	(Richardson et al., 2007)
Excess Green	ExG=2xG-R-B	(Woebbecke et al., 1995)
Green Leaf Index	GLI=((G-R)+(G-B))/(2G+R+B)	(Louhaichi et al., 2001)
Red Green Blue Vegetation Index	$RGBVI=(G^2-(BxR))/(G^2+(BxR))$	(Bendig et al., 2015)
Triangular Greenness Index	TGI=G-0.39xR-0.61xB	(Hunt et al., 2011)
Modified Green Red Vegetation Index	$MGRVI=(G^2-R^2)/(G^2+R^2)$	(Bendig et al., 2015)

R – red
G – green
B – blue
NIR – Near Infrared
*a – slope of the ground line
*b – gradient of the ground line
Re – Red edge
**rb = R-γ(B-R), γ – variable dependent on the type of aerosols present in the atmosphere and takes the value of 1 when there is no information about the type of aerosols. The purpose of "rb" is to reduce atmospheric influence in order to achieve a more accurate assessment of the red band reflectance value.
***R_{665} = Band 4 Sentinel 2 - Red
***Re_{705} = Band 5 Sentinel 2 – Vegetation Red Edge
***Re_{740} = Band 6 Sentinel 2 – Vegetation Red Edge
***Re_{783} = Band 7 Sentinel 2 – Vegetation Red Edge

A subset of vegetation indices (NDRE, IRVI, GRVI, VREI, MPRI, VARI, GPI, ExG, GLI, RGBVI, TGI, MGRVI) were calculated using the *Raster Calculator function (Spatial Analyst Tools – Map Algebra)* within the *ArcGIS* software, while another subset (NDVI, SAVI, MSAVI2, DVI, RVI, PVI, IPVI, WDVI, TNDVI, GNDVI, ARVI, NDI45, IRECI, PSSRa) were automatically provided by the *SNAP program (ESA Sentinel Application Platform v8.0)*, which facilitates direct acquisition of vegetation index values based on spectral information.

For each obtained biophysical and vegetation index, the average pixel values were calculated for each one hectare sample area using the *Zonal Statistics as Table function (Spatial Analyst Tools – Zonal)* within the *ArcGIS* software. Based on the average level of defoliation or discoloration assessed in the field, as well as the average pixel values for each sample area, mathematical relationships were established between the observed damage values and pixel values. This was achieved through the application of the *Multiple Regression* and *Analysis of Variance* methods using the specialized software *Statistica 12.0*.

Processing these images in the form of biophysical and vegetation indices enabled the establishment of ranges of pixel values for each level of damage. Based on these pixel value ranges, thematic maps were created to depict the extent of damages, and these maps were compared to thematic maps obtained from ground-recorded data. The thematic maps generated using biophysical and vegetation indices were produced using *ArcGIS* software. This was achieved through reclassifying the digital images (using the *Reclassify function* within the *3D Analyst Tools* module) that represent the respective indices according to the specific pixel value ranges associated with each level of damage.

Based on the obtained thematic maps, both from field observations and biophysical and vegetation indices, the areas affected by defoliation or discoloration were determined in different levels of damage. This was achieved using the *Raster to Polygon function* within the *Conversion Tools* module of *ArcGIS* software. The purpose was to conduct a comparative analysis of the extent of damages.

4. RESULTS AND DISCUSSION

4.1. Monitoring and assessment of damages (defoliation) caused by *Lymantria dispar*

4.1.1. Quantitative and qualitative characteristics of *Lymantria dispar* populations and assessment, on field, of the damages caused by them

Starting from the year 2018, the defoliator *Lymantria dispar* has experienced a population increase in the southern area of the Oltenia Plain, infesting numerous forest stands, particularly those composed mainly of turkey oak and hungarian oak species, like the Ciuturica forest stand, which was selected as the experimental area for the research objectives.

In the 2019-2020 generation, the population of *Lymantria dispar* was in the phase of numerical growth, with an average fecundity of 684 eggs, 7% of which were parasitized in the egg stage, 2.4% sterility rate, and an average density of 1.98 egg masses per tree, ranging from 0.1 to 4.9 egg masses per tree (with a coefficient of variation of 61.1%), depending on the forest stand characteristics and structure. Based on the determined quantitative and qualitative characteristics, an average defoliation of 169% was forecasted, with variations ranging from 5% to 405% from tree to tree (with a coefficient of variation of 14.78%). Due to the spatial homogenization of infestations caused by wind action on the young larval stage and natural mortality, the actual defoliation was much lower than predicted, with an average of 23.4% and variations ranging from 6% to 49% (with a coefficient of variation of 16.93%).

For the 2020-2021 generation, the population of *Lymantria dispar* evolved from the phase of numerical growth to the outbreak phase, with an average fecundity of 495.75 eggs, 11% of which were parasitized in the egg stage, 4.2% sterility rate, and an average density of 19.77 egg masses per tree, ranging from 0.5 to 49 egg masses per tree (with a coefficient of variation of 43.7%), depending on the forest stand characteristics and structure. Based on the determined quantitative and qualitative characteristics, an average defoliation of 293% was forecasted, with variations ranging from 1% to 622% from tree to tree (with a coefficient of variation of 14.29%). In the spring of 2021, due to strong and very strong infestations throughout the forest stand, aerial treatments were applied, leading to a reduction in actual defoliation compared to the forecasted values, down to 12.4%, with variations ranging from 1% to 22% (with a coefficient of variation of 18.09%).

Due to the very high level of infestation from previous generations, after the aerial treatments were applied, in the 2021-2022 generation, a residual population remained in a crisis phase. This population had an average fecundity of 418 eggs, with 9.33% parasitization in the egg stage, 8.67% sterility rate, and an average density of 0.013 egg masses per tree, ranging from 0.01 to 0.025 egg masses per tree (with a coefficient of variation of 27.77%), depending on the forest stand characteristics and structure. Based on the determined quantitative and qualitative characteristics, an average defoliation of 1.17% was forecasted, with variations ranging from 0% to 9% from tree to tree (with a coefficient of variation of 8.02%). The actual average defoliation achieved was 3.83%, with variations from 0% to 10% (with a coefficient of variation of 13.39%).

Based on the data regarding the degrees of realized defoliation recorded within the rectangular network of sample circles, thematic maps were created to depict the spatial distribution of damages based on defoliation degrees for the 2019-2020 generation (figure 9a) and the 2020-2021 generation (figure 9b).

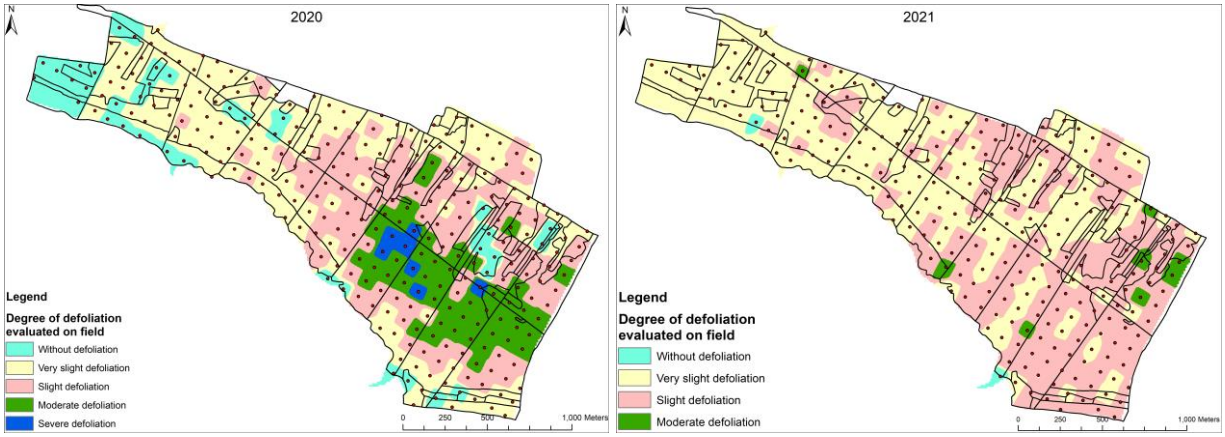

a b

Figure 9. Thematic maps with the spatial distribution of defoliation produced by *Lymantria dispar*, by degree of intensity, for the 2019-2020 generation (a) and the 2020-2021 generation (b), in the Ciuturica forest stand

4.1.2. Assessment of defoliation produced by *Lymantria dispar* based on Sentinel 2 satellite images

4.1.2.1. Assessment of defoliation produced by *Lymantria dispar* based on biophysical indices

Based on Sentinel 2 satellite images obtained for the Ciuturica forest stand, at the phenological stage after the feeding of *Lymantria dispar* caterpillars stopped (last decade of July) for the 2019-2020 and 2020-2021 generations, all five biophysical indices offered by the *ESA Snap* program were determined. These indices are based on the generation of databases with vegetation characteristics and spectral reflectance from the upper part of the tree canopy, as highlighted in figure 13.

Using the pixel value series provided by the *ArcGIS* program through the *Zonal Statistics as Table function (Spatial Analyst Tools - Zonal)*, mean values and indices of dispersion were established for each biophysical index. Additionally, through simple regression analysis, the correlation between the realized defoliations, evaluated in the field for each sampled area, in the two vegetation seasons (2020, 2021), and the average pixel values from the respective areas, was determined for each biophysical index (table 3).

Table no. 3. Basic statistical parameters of the biophysical indices obtained and the correlation between pixel values and defoliation by *Lymantria dispar* in two consecutive generations

Biophysical indices	Basic statistical parameters for year									
	2020					2021				
	Mean	St. dev.	Coeff. of variation (%)	Coeff. of correlation (r)	Level of significance (p)	Mean	St. dev.	Coeff. of variation (%)	Coeff. of correlation (r)	Level of significance (p)
LAI	2.698	0.313	11.59	-0.609	$2.2x10^{-8}$	2.217	0.223	10.07	-0.587	$9x10^{-8}$
FAPAR	0.716	0.045	6.32	-0.599	$4.2x10^{-8}$	0.655	0.037	5.65	-0.565	$3.5x10^{-7}$
FVC	0.649	0.051	7.87	-0.608	$2.4x10^{-8}$	0.604	0.038	6.31	-0.557	$5.6x10^{-7}$
CAB	106.350	21.438	20.16	-0.672	$1.9x10^{-10}$	91.338	13.631	14.92	-0.572	$2.3x10^{-7}$
CWC	0.033	0.005	16.17	-0.748	$1x10^{-13}$	0.037	0.003	7.95	-0.620	$1x10^{-8}$

The analysis of the information presented in table 3 indicates that all obtained biophysical indices for the two defoliation years have low coefficients of variation, implying that pixel values have a reduced degree of dispersion. Additionally, there is a strong and highly significant relationship ($p<0.001$) between the respective statistical series (pixel values series and defoliation values series), with correlation coefficients ranging from 0.60 to 0.75 for the year 2020 and 0.56 to 0.62 for the year 2021.

By conducting simple variance analysis, standard errors and the range of variation from the mean pixel values within the sampled areas were calculated for each biophysical index, across defoliation degrees, for the two consecutive years (table 4).

Table no. 4. Range of variation of pixel values for biophysical indices, relative to standard error

Defoliation degree	2020				2021				Pixel variation range 2020-2021
	$\bar{X}$	$\sigma_{\bar{x}}$	$\bar{X}$-$\sigma_{\bar{x}}$ (min)	$\bar{X}$+$\sigma_{\bar{x}}$ (max)	$\bar{X}$	$\sigma_{\bar{x}}$	$\bar{X}$-$\sigma_{\bar{x}}$ (min)	$\bar{X}$+$\sigma_{\bar{x}}$ (max)	($\bar{X}$-$\sigma_{\bar{x}}$; $\bar{X}$+$\sigma_{\bar{x}}$)
CWC									
very slight	0.037	0.001	**0.037**	**0.038**	0.039	0.0004	**0.038**	**0.039**	**0.037-0.039**
slight	0.032	0.001	**0.032**	**0.033**	0.035	0.0004	**0.035**	**0.036**	**0.032-0.036**
moderate	0.027	0.001	**0.026**	**0.028**					**0.026-0.028**

The data analysis regarding the range of variation of pixel values in the two years with defoliation shows that some biophysical indices (LAI, FAPAR, FVC, CAB) exhibit varying levels of overlap between defoliation degrees (e.g. for LAI, there is overlap between the very slight and slight defoliation degrees in the range 2.30-2.74, and between the slight and moderate defoliation degreess in the range 2.29-2.43). For the CWC index, the ranges of pixel values in the two years are distinct, suggesting a higher degree of stability for this index in assessing the defoliation caused by *Lymantria dispar*.

4.1.2.2. Assessment of defoliation produced by *Lymantria dispar* based on vegetation indices calculated in the near infrared range (NIR)

Using satellite imagery and mathematical operations between various spectral bands, especially near-infrared, red, green, and blue, a series of vegetation indices have been calculated. These indices are based on the vegetation's ability to absorb maximum energy in the red and blue bands and strong reflectance in the near-infrared band. Some of these vegetation indices were obtained using the *ESA Snap* program (NDVI, SAVI, MSAVI2, DVI, RVI, PVI, IPVI, WDVI, TNDVI, GNDVI, ARVI, NDI45, IRECI, and PSSRa), while others were calculated using *ArcGIS* software (NDRE, IRVI, GRVI, and VREI). These calculations were performed for the Ciuturica forest stand at the phenological moment after the feeding of *Lymantria dispar* caterpillars had ceased (last decade of July) for the 2019/2020 and 2020/2021 generations.

For each vegetation index, based on the series of pixel values provided by the *ArcGIS* program using the *Zonal Statistics as Table function (Spatial Analyst Tools - Zonal)*, mean values and dispersion indices were determined. Additionally, through a simple regression analysis, the correlation between realized defoliation levels, assessed in the field for each investigated sample area in the two vegetation seasons (2020, 2021), and the mean pixel values from the respective areas were established for each index separately (table 5).

Table no. 5. Basic statistical parameters of the vegetation indices obtained in near – infrared (NIR) and the correlation between pixel values and defoliation by *Lymantria dispar* in two consecutive generations

Vegetation indices	Basic statistical parameters for year ……									
	2020					2021				
	Mean	Std. dev.	Coeff. of variation (%)	Coeff. of correlation (r)	Level of significance (p)	Mean	Std. dev.	Coeff. of variation (%)	Coeff. of correlation (r)	Level of significance (p)
NDVI	0.821	0.026	3.12	-0.538	**$1.5x10^{-6}$**	0.738	0.024	3.27	-0.553	**$6.8x10^{-7}$**
SAVI	0.490	0.032	6.56	-0.602	**$3.6x10^{-8}$**	0.464	0.022	4.74	-0.539	**$1.4x10^{-6}$**
MSAVI2	0.438	0.035	8.03	-0.607	**$2.6x10^{-8}$**	0.415	0.023	5.55	-0.538	**$1.6x10^{-7}$**
DVI	0.272	0.025	8.99	-0.613	**$1.7x10^{-8}$**	0.267	0.016	6.01	-0.516	**$4.9x10^{-6}$**
RVI	10.637	1.693	15.91	-0.550	**$8.1x10^{-7}$**	6.747	0.709	10.51	-0.564	**$3.6x10^{-7}$**
PVI	0.192	0.017	8.82	-0.594	**$5.8x10^{-8}$**	0.189	0.011	6.01	-0.516	**$4.8x10^{-6}$**
IPVI	0.911	0.013	1.41	-0.538	**$1.5x10^{-6}$**	0.869	0.012	1.39	-0.553	**$6.8x10^{-7}$**
WDVI	0.258	0.026	9.91	-0.611	**$1.9x10^{-8}$**	0.243	0.017	6.95	-0.544	**$1.1x10^{-6}$**
TNDVI	1.149	0.011	0.97	-0.537	**$1.6x10^{-6}$**	1.113	0.011	0.98	-0.553	**$7.1x10^{-7}$**
GNDVI	0.732	0.026	3.6	-0.577	**$1.7x10^{-7}$**	0.670	0.024	3.5	-0.521	**$3.8x10^{-6}$**
ARVI	0.809	0.034	4.21	-0.545	**$1x10^{-6}$**	0.682	0.033	4.8	-0.558	**$5.2x10^{-7}$**
NDI45	0.443	0.023	5.2	-0.290	$1.4x10^{-2}$	0.362	0.014	3.77	-0.426	**$2.4x10^{-4}$**

IRECI	0.905	0.166	18.31	-0.596	$5.2x10^{-8}$	0.656	0.088	13.39	-0.550	$8.2x10^{-7}$
PSSRa	10.637	1.693	15.91	-0.550	$8.1x10^{-7}$	6.747	0.709	10.51	-0.564	$3.6x10^{-7}$
NDRE	0.598	0.037	6.16	-0.602	$3.5x10^{-8}$	0.111	0.007	6.59	-0.489	$1.7x10^{-5}$
IRVI	0.099	0.016	15.84	0.535	$1.9x10^{-6}$	0.151	0.016	10.62	0.551	$7.6x10^{-7}$
GRVI	6.637	0.763	11.49	-0.577	$1.7x10^{-7}$	5.228	0.439	8.39	-0.530	$2.4x10^{-6}$
VREI	1.228	0.026	2.14	-0.687	$5.1x10^{-11}$	1.251	0.018	1.46	-0.495	$1.3x10^{-5}$

From the analysis of the information presented in table 5, it can be observed that all the vegetation indices determined in the near-infrared (NIR) domain for the two defoliation years have low coefficients of variation, indicating that the pixel values exhibit a reduced level of dispersion. Additionally, a close and highly significant relationship ($p<0.001$) is observed between most of the statistical series (pixel values and defoliation values), with correlation coefficients ranging between 0.29-0.69 for the year 2020 and 0.43-0.56 for the year 2021.

Through the simple variance analysis, standard errors and the range of variation relative to the mean pixel values from the sampled areas were calculated for each vegetation index determined based on the near-infrared (NIR) band, across different defoliation degrees, for the two consecutive years (2020-2021) (table 6).

Table no. 6. Range of variation of pixel values for vegetation indices obtained in near – infrared (NIR), relative to standard error

Defoliation degree	2020				2021				Pixel variation range 2020-2021
	$\bar{X}$	$\sigma_{\bar{X}}$	$\bar{X}-\sigma_{\bar{X}}$ (min)	$\bar{X}+\sigma_{\bar{X}}$ (max)	$\bar{X}$	$\sigma_{\bar{X}}$	$\bar{X}-\sigma_{\bar{X}}$ (min)	$\bar{X}+\sigma_{\bar{X}}$ (max)	$(\bar{X}-\sigma_{\bar{X}}; \bar{X}+\sigma_{\bar{X}})$
DVI									
very slight	0.285	0.004	0.281	0.288	0.275	0.002	0.273	0.278	**0.273-0.288**
slight	0.271	0.004	0.267	0.275	0.259	0.002	0.257	0.262	**0.257-0.275**
moderate	0.245	0.005	0.240	0.250					**0.240-0.250**
PVI									
very slight	0.201	0.002	0.198	0.203	0.195	0.002	0.193	0.196	**0.193-0.203**
slight	0.192	0.003	0.189	0.195	0.183	0.002	0.182	0.185	**0.182-0.195**
moderate	0.174	0.004	0.170	0.177					**0.170-0.177**
VREI									
very slight	1.245	0.003	1.242	1.249	1.258	0.003	1.255	1.261	**1.242-1.261**
slight	1.221	0.004	1.217	1.225	1.245	0.003	1.242	1.248	**1.217-1.248**
moderate	1.199	0.005	1.194	1.204					**1.194-1.204**

The data analysis regarding the range of variation of pixel values in the two years with defoliation shows that vegetation indices such as NDVI, SAVI, MSAVI2, RVI, IPVI, WDVI, TNDVI, GNDVI, ARVI, NDI45, IRECI, PSSRa, NDRE, IRVI, and GRVI exhibit varying levels of overlap between the "very slight" and "slight" defoliation degrees, "slight" and "moderate" defoliation degrees, and even between the "very slight" and "moderate" defoliation degrees. On the other hand, for vegetation indices DVI, PVI, and VREI, the ranges of pixel values in the two years are distinct, showing small overlaps (0.002 for DVI and PVI, and 0.006 for VREI) between the "very slight" and "slight" defoliation degrees. *This suggests a higher degree of stability for these indices in assessing defoliation caused by Lymantria dispar*.

4.1.2.3. Assessment of defoliation produced by *Lymantria dispar* based on vegetation indices calculated in the visible range (RGB)

Based on the satellite images, a series of vegetation indices were calculated through mathematical operations involving the red, green, and blue spectral bands. These vegetation indices were determined using the *ArcGIS* software for the Ciuturica forest stand at the phenological moment following the cessation of *Lymantria dispar* caterpillar feeding (last decade of July) in the 2019-2020 and 2020-2021 generations.

For each vegetation index, the mean values and dispersion indices were determined. Additionally, through a simple regression analysis, the correlation between the realized defoliation levels evaluated in the field for each sampled area and the average pixel values in those respective areas during the two vegetation seasons (2020, 2021) were established (table 7).

Table no. 7. Basic statistical parameters of the vegetation indices obtained in visible range (RGB) and the correlation between pixel values and defoliation by *Lymantria dispar* in two consecutive generations

Vegetation indices	Basic statistical parameters for year ……									
	2020					2021				
	Mean	Std. dev.	Coeff. of variation (%)	Coeff. of correlation (r)	Level of significance (p)	Mean	Std. dev.	Coeff. of variation (%)	Coeff. of correlation (r)	Level of significance (p)
MPRI	0.226	0.027	12.01	-0.370	**$1.6x10^{-3}$**	0.110	0.012	11.06	-0.497	**$1.2x10^{-5}$**
VARI	0.353	0.045	12.76	-0.403	**$5.4x10^{-4}$**	0.185	0.024	12.79	-0.505	**$8.4x10^{-6}$**
GPI	0.451	0.009	2.04	-0.236	**$5.0x10^{-2}$**	0.424	0.005	1.28	-0.376	**$1.3x10^{-3}$**
ExG	356.402	26.751	7.51	0.077	$5.3x10^{-1}$	387.214	32.184	8.31	0.055	$6.5x10^{-1}$
GLI	0.242	0.018	7.21	-0.234	**$5.1x10^{-2}$**	0.191	0.011	5.62	-0.377	**$1.3x10^{-3}$**
RGBVI	0.458	0.029	6.24	-0.223	$6.4x10^{-2}$	0.378	0.019	4.91	-0.335	**$4.5x10^{-3}$**
TGI	180.658	13.575	7.51	0.140	$2.4x10^{-1}$	206.942	17.516	8.46	0.118	$3.3x10^{-1}$
MGRVI	0.427	0.047	10.9	-0.368	**$1.7x10^{-3}$**	0.245	0.029	11.89	-0.497	**$1.2x10^{-5}$**

From the analysis of the information in Table 7, it can be observed that all vegetation indices determined in the visible domain (RGB) for the two years with defoliation have low coefficients of variation, indicating that pixel values have a reduced degree of dispersion. Additionally, weak but significant correlations ($p<0.001$) were found only for the vegetation indices MPRI, VARI, and MGRVI. These correlations, which exist between the statistical series (the series of pixel values and the series of defoliation values), have correlation coefficients ranging from 0.08 to 0.40 for the year 2020 and from 0.06 to 0.51 for the year 2021.

Through the simple variance analysis were calculated the standard errors and the range of variation relative to the mean pixel values from the sampled areas for each vegetation index determined in the visible domain (RGB), based on different degrees of defoliation in the two consecutive years (2020-2021).

The analysis of data regarding the range of variation of pixel values in the two years with defoliation shows that all studied vegetation indices (MPRI, VARI, GPI, ExG, GLI, RGBVI, TGI, MGRVI) exhibit varying levels of overlap between the degrees of defoliation categorized as very slight and slight, slight and moderate, and very slight and moderate. *This suggests that these indices may not be suitable for accurately assessing defoliation caused by Lymantria dispar.*

4.1.2.4. Comparative analysis of the results of defoliation assessments established on field, with those obtained from satellite images

The thematic maps obtained for the evaluation of defoliation results recorded through field assessments in the two years (2020 and 2021), caused by the *Lymantria dispar* defoliator and presented in section 4.1.1., have enabled the determination of the affected areas based on defoliation degrees (figure 10a). Additionally, the thematic maps derived from biophysical and vegetation indices, calculated using intervals of pixel value variation specific to each defoliation degree and statistically proven to have significant influence (CWC, DVI, PVI, VREI), have facilitated the calculation of areas according to the established defoliation degrees corresponding to the ranges of pixel values (figure 10b, c, d, e).

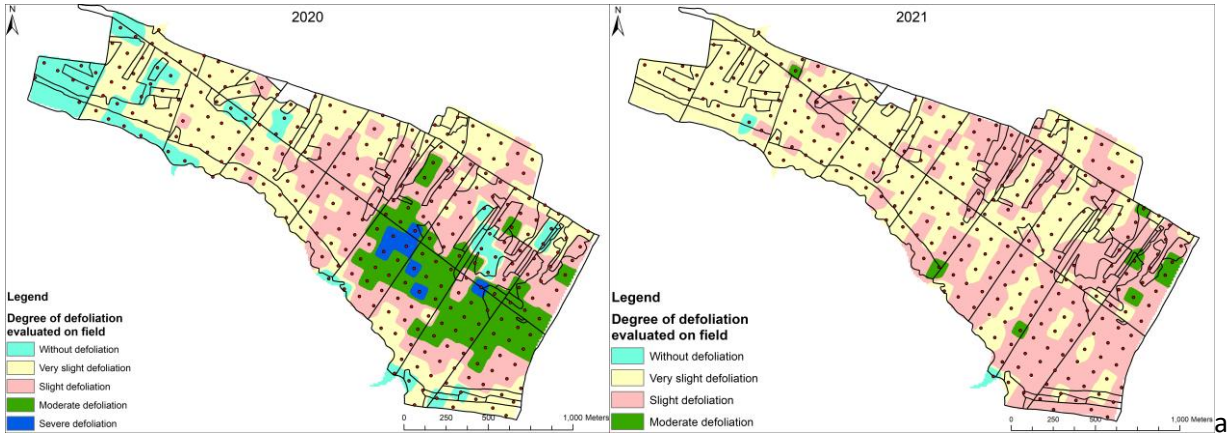
2020
2021
Legend
Degree of defoliation evaluated on field
Without defoliation
Very slight defoliation
Slight defoliation
Moderate defoliation
Severe defoliation
0 250 500 1,000 Meters

a

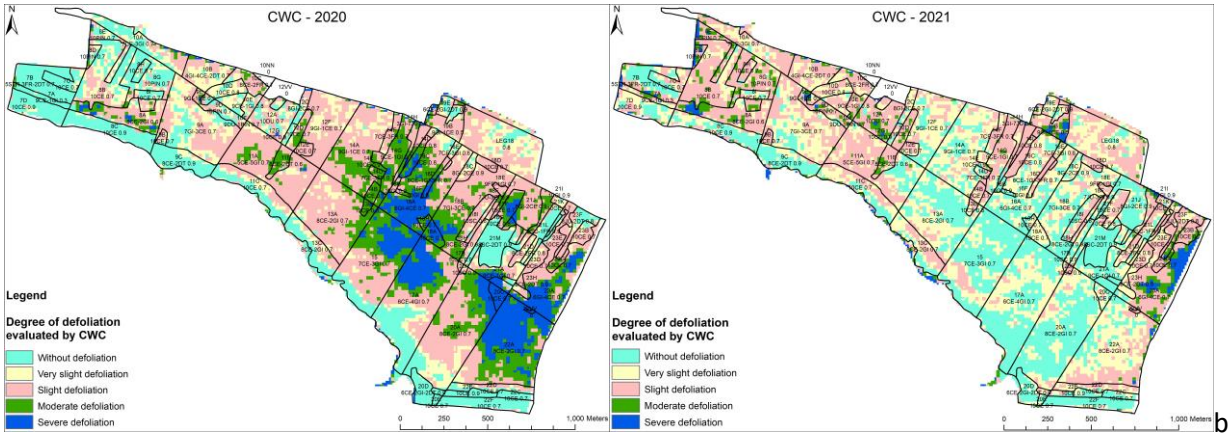
CWC - 2020
CWC - 2021
Legend
Degree of defoliation evaluated by CWC
Without defoliation
Very slight defoliation
Slight defoliation
Moderate defoliation
Severe defoliation
0 250 500 1,000 Meters

b

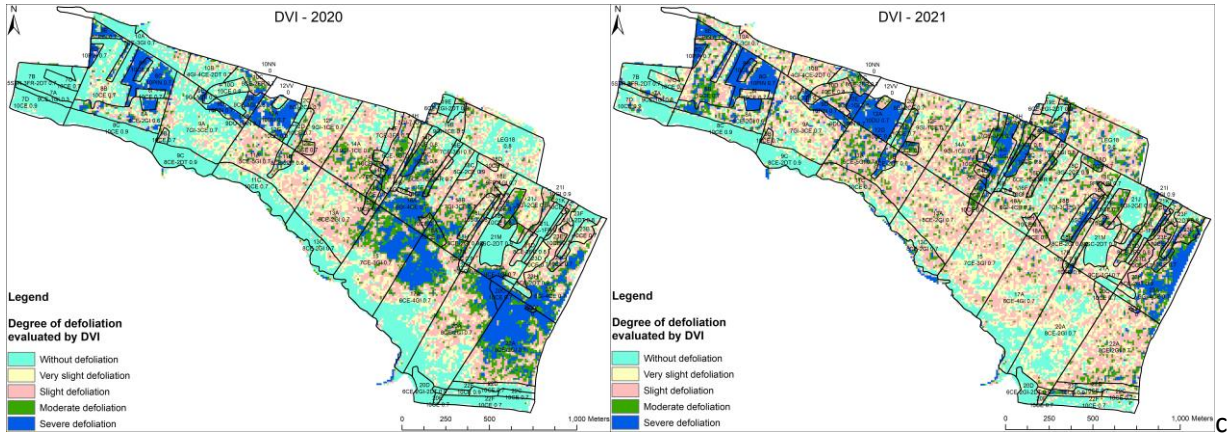
DVI - 2020
DVI - 2021
Legend
Degree of defoliation evaluated by DVI
Without defoliation
Very slight defoliation
Slight defoliation
Moderate defoliation
Severe defoliation
0 250 500 1,000 Meters

c

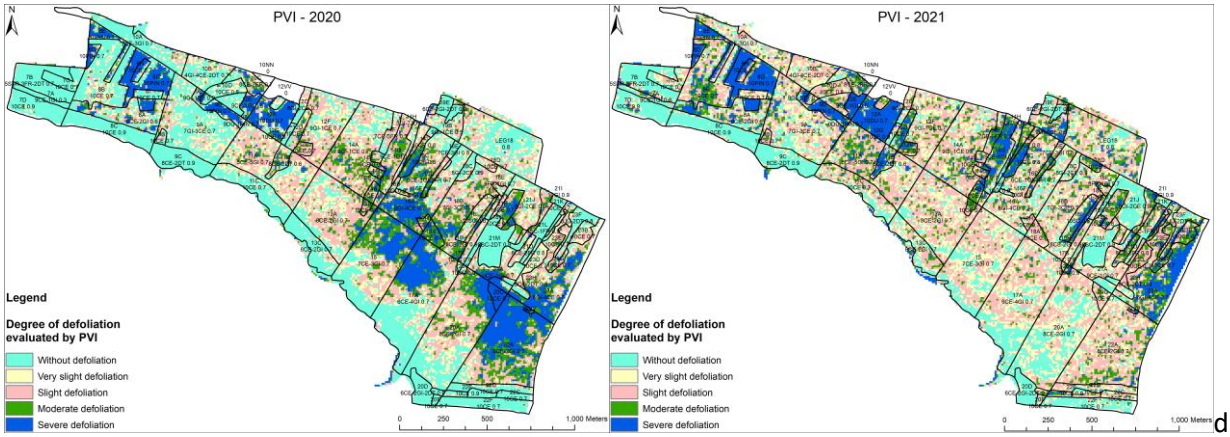
PVI - 2020
PVI - 2021
Legend
Degree of defoliation evaluated by PVI
Without defoliation
Very slight defoliation
Slight defoliation
Moderate defoliation
Severe defoliation
0 250 500 1,000 Meters

d

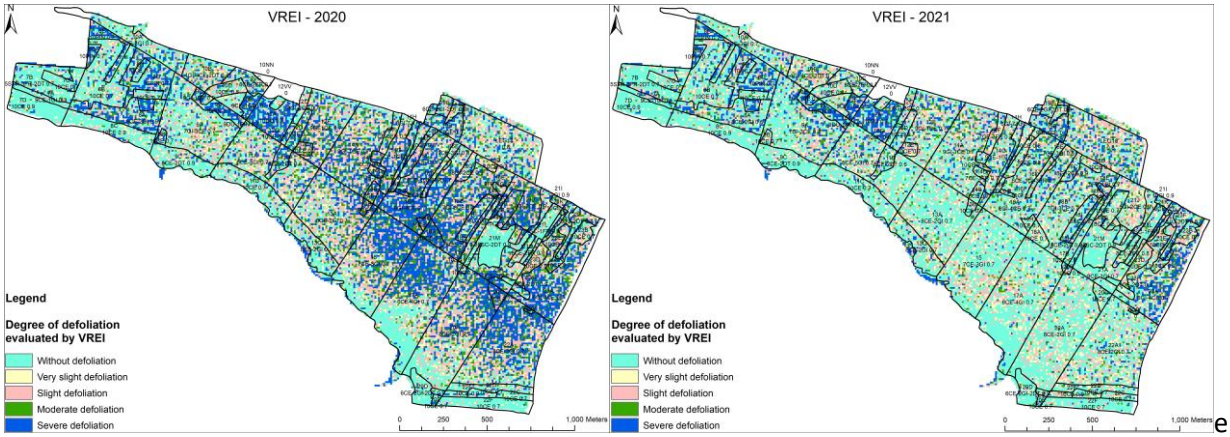

Figure 10. Thematic maps obtained based on ground assessments and biophysical (CWC) and vegetation (DVI, PVI, VREI) indices for the years 2020 and 2021

The visual comparison of the two types of thematic maps (field observations and satellite imagery) reveals that among all statistically proven significant indices, the biophysical index CWC, which estimates leaf water content per unit area, provided the closest spatial distribution of defoliation degrees to the field observation results for the year 2020. For the year 2021, it was observed that this index still exhibited a similar trend of approximation to the field thematic map, although reduced due to the significantly lower defoliation level compared to the previous year. These variations in the trend between the two years, as indicated by the CWC index, could be attributed to the subjectivity of field operators, who tend to overestimate very slight-intensity damages. Thematic maps obtained using other vegetation indices (DVI, PVI, and VREI), which were statistically proven to be significant, do not capture the distribution of defoliation degrees across the forest area to the same extent.

The comparative analysis of the areas categorized by defoliation degrees on the thematic maps generated based on pixel value ranges for the biophysical index CWC and the vegetation indices DVI, PVI, and VREI, as well as those obtained from field observations, revealed differences between the estimated field-based defoliation areas and those calculated based on the indices. These differences were observed across the different indices as follows (figure 11):

- the areas considered as unaffected by defoliation, calculated based on each of the studied indices, *were larger than those calculated from ground observations.*

- the areas classified as slight and moderate affected by defoliation, calculated based on each of the studied indices, *were notably smaller compared to those calculated from ground observations.*

- the areas classified as moderate and severe affected by defoliation, calculated based on each of the studied indices, *were larger than those calculated from ground observations.*

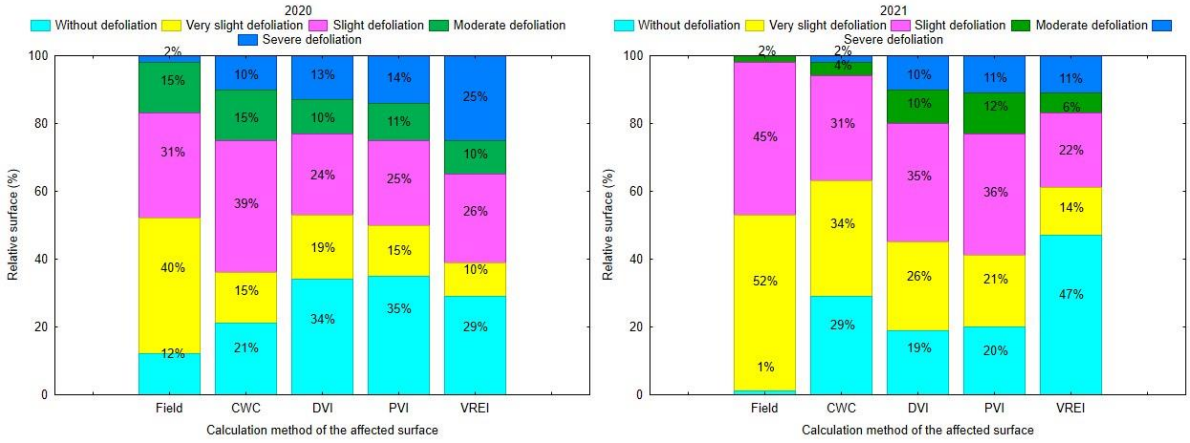

Figure 11. The comparative variation of the relative surfaces, by degrees of defoliation, calculated, on the thematic maps, obtained according to the data recorded from the field and those obtained based on the indices (Field, CWC, DVI, PVI, VREI)

Differences in the underestimated areas for zones without defoliation on the field-based thematic maps may partially be explained by the subjectivity of field operators, who may tend to categorize non-

defoliated trees as slightly defoliated. Furthermore, the differences observed in the overestimated areas on the thematic maps obtained from indices compared to those calculated from field-based data can be explained by systematic errors in defoliation underestimation by operators. These operators may not always capture the upper part of the crown, which is often the most affected, in their visual field. In contrast, satellite and aerial digital images can better capture this upper part, resulting in more accurate assessments.

The visual analysis as well as the integrated analysis based on the calculation of areas covered by the two types of thematic maps indicate that the biophysical index CWC best captures both the areas without defoliation and those affected by different degrees of defoliation caused by *Lymantria dispar*.

4.1.3. Assessment of defoliation produced by *Lymantria dispar* based on aerial images captured with the drone

4.1.3.1. Assessment of defoliation produced by *Lymantria dispar* based on vegetation indices calculated in the visible range (RGB)

On the aerial images obtained using a drone, several vegetation indices (MPRI, VARI, GPI, ExG, GLI, RGBVI, TGI, MGRVI) were calculated through algorithms based on the red, green, and blue spectral bands, with the aim of creating thematic maps that highlight areas affected by defoliation in various degrees. These vegetation indices were determined using the *ArcGIS* software for a portion of the Ciuturica forest stand, at a phenological stage following the cessation of *Lymantria dispar* caterpillar feeding (last decade of July) during the 2019-2020 and 2020-2021 generations.

For each vegetation index, the main statistical parameters (mean, standard deviation, and coefficient of variation) of the statistical series formed by the pixel values from the one hectare sample areas were calculated for the two vegetation seasons (2020, 2021) (table 8). Additionally, through simple regression analysis, the correlation between the defoliations observed in the field and the average pixel values from the respective areas was determined for each index.

Table nr. 8. Basic statistical parameters of the vegetation indices obtained in visible range (RGB) and the correlation between pixel values and defoliation by *Lymantria dispar* in two consecutive generations

Vegetation indices	Basic statistical parameters for year ……									
	2020					2021				
	Mean	Std. dev.	Coeff. of variation (%)	Coeff. of correlation (r)	Level of significance (p)	Mean	Std. dev.	Coeff. of variation (%)	Coeff. of correlation (r)	Level of significance (p)
MPRI	0.085	0.021	24.6	-0.647	**$1.1x10^{-4}$**	0.108	0.023	21.35	-0.622	**$2.5x10^{-4}$**
VARI	0.138	0.038	27.76	-0.648	**$1.1x10^{-4}$**	0.209	0.051	24.53	-0.633	**$1.7x10^{-4}$**
GPI	0.394	0.005	1.37	-0.308	$9.8x10^{-2}$	0.386	0.006	1.55	-0.355	$5.4x10^{-2}$
ExG	70.957	5.202	7.3	-0.083	$6.6x10^{-1}$	32.885	3.477	10.57	0.244	$1.9x10^{-1}$
GLI	0.130	0.011	8.49	-0.304	$1x10^{-1}$	0.113	0.012	10.9	-0.357	$5.3x10^{-2}$
RGBVI	-0.366	0.011	-2.93	-0.224	$2.4x10^{-1}$	0.228	0.024	10.32	-0.360	$5.1x10^{-2}$
TGI	38.094	2.905	7.63	0.138	$4.7x10^{-1}$	29.188	2.537	8.69	-0.293	$1.1x10^{-1}$
MGRVI	0.168	0.041	24.13	-0.647	**$1.1x10^{-4}$**	0.210	0.043	20.66	-0.616	**$2.9x10^{-4}$**

From the analysis of the information presented in table 8, it can be observed that all vegetation indices determined in the visible domain (RGB) for the two defoliation years exhibit low coefficients of variation, indicating a reduced degree of pixel value dispersion. Additionally, a strong, highly significant relationship ($p<0.001$) is evident between the statistical series (series of pixel values and series of defoliation values) for the vegetation indices MPRI, VARI, and MGRVI. The correlation coefficients are around 0.65 for the year 2020 and range between 0.62 and 0.63 for the year 2021.

Through the simple variance analysis, standard errors and the range of variation relative to the mean pixel values within the sampled areas were calculated for each vegetation index determined in the visible domain (RGB), according to different defoliation degrees, over the two consecutive years (2020-2021) (table 9).

Table no. 9. Range of variation of pixel values for vegetation indices obtained in visible domain (RGB), relative to standard error

Defoliation degree	2020				2021				Pixel variation range 2020-2021
	$\bar{X}$	$\sigma_{\bar{x}}$	$\bar{X}$-$\sigma_{\bar{x}}$ (min)	$\bar{X}$+$\sigma_{\bar{x}}$ (max)	$\bar{X}$	$\sigma_{\bar{x}}$	$\bar{X}$-$\sigma_{\bar{x}}$ (min)	$\bar{X}$+$\sigma_{\bar{x}}$ (max)	($\bar{X}$-$\sigma_{\bar{x}}$; $\bar{X}$+$\sigma_{\bar{x}}$)
MPRI									
very slight	0.110	0.007	0.103	0.117	0.119	0.007	0.112	0.125	**0.103-0.125**
slight	0.088	0.004	0.084	0.092	0.101	0.005	0.096	0.106	**0.084-0.106**
moderate	0.070	0.005	0.065	0.075					**0.065-0.075**
MGRVI									
very slight	0.216	0.014	0.202	0.230	0.230	0.012	0.218	0.243	**0.202-0.243**
slight	0.174	0.008	0.166	0.182	0.198	0.009	0.189	0.207	**0.166-0.207**
moderate	0.139	0.009	0.129	0.148					**0.129-0.148**

The analysis of data from table 9 regarding the range of variation of pixel values in the two years with defoliation reveals that vegetation indices such as VARI, GPI, ExG, GLI, RGBVI, and TGI exhibit varying levels of overlap between the categories of very slight, slight, and moderate defoliation. On the other hand, for the vegetation indices MPRI and MGRVI, the ranges of pixel value variation are distinct in the two years, showing minimal overlap (0.004 for MPRI and 0.006 for MGRVI) between the degrees of very slight and slight defoliation. This suggests a higher level of stability for these indices in assessing defoliation caused by *Lymantria dispar*, *indicating that MPRI and MGRVI indices are better suited for capturing defoliation caused by Lymantria dispar compared to other vegetation indices within this category.*

4.1.3.2. Assessment of defoliation produced by *Lymantria dispar* based on vegetation indices calculated in the visible range (RGB), for individual trees

For a more detailed analysis of the additional information provided by high-resolution images captured using a drone in the year 2020, when defoliation degrees were higher, field assessments were conducted for the 70 individual trees categorized into various degrees of defoliation. These trees were located within the drone's flight polygon.

Based on these images, the same vegetation indices as presented in chapter 4.1.3.1 were calculated using algorithms that utilize red, green, and blue spectral bands (MPRI, VARI, GPI, ExG, GLI, RGBVI, TGI, MGRVI).

For each vegetation index, the main statistical parameters (mean, standard deviation, coefficient of variation) were determined for the statistical series consisting of pixel values specific to the crown area of each tree at the post-defoliation moment. Additionally, the correlation between the defoliations assessed in the field and the average pixel values of the crown areas of individual trees was established (table 10).

Table no. 10. Basic statistical parameters of the vegetation indices obtained in visible range (RGB) and the correlation between pixel values and defoliation by *Lymantria dispar* in generation 20119-2020

Vegetation indices	Mean	Std. dev.	Coeff. of variation (%)	Regression equation	Coeff. of correlation (r)	Level of significance (p)
MPRI	0.064	0.024	38.112	Def. (%)=103.47-938.1*MPRI	-0.781	**$1.6x10^{-15}$**
VARI	0.100	0.038	37.385	Def. (%)=103.20-597.5*VARI	-0.763	**$1.7x10^{-14}$**
GPI	0.391	0.013	3.356	Def. (%)=689.14-1653*GPI	-0.738	**$3.0x10^{-13}$**
ExG	74.437	18.161	24.398	Def. (%)=127.76-1.134*ExG	-0.702	**$1.3x10^{-11}$**
GLI	0.124	0.027	21.960	Def. (%)=142.03-799.2*GLI	-0.739	**$2.9x10^{-13}$**
RGBVI	-0.371	0.027	-7.206	Def. (%)=248.8-787.8*RGBVI	-0.717	**$2.8x10^{-12}$**
TGI	40.955	9.671	23.614	Def. (%)=125.7-2.011*TGI	-0.663	**$4.2x10^{-10}$**
MGRVI	0.127	0.048	37.808	Def. (%)=103.99-476.2*MGRVI	-0.781	**$1.6x10^{-15}$**

There are linear relationships between the pixel values obtained from all calculated vegetation indices and the field-estimated defoliations, characterized by negative correlation coefficients of moderate intensity (GPI, ExG, GLI, RGBVI, TGI) and strong intensity (MPRI, VARI, MGRVI), which are highly significant.

Through the simple variance analysis, the standard errors and the range of variation around the mean pixel values for the sampled tree canopies were calculated for each vegetation index, determined in the visible domain (RGB), across defoliation degrees in the 2019-2020 generation (table 11).

Table no. 11. Range of variation of pixel values for vegetation indices obtained in visible domain (RGB), relative to standard error

Defoliation degree	$\bar{X}$	$\sigma_{\bar{X}}$	Pixel variation range		$\bar{X}$	$\sigma_{\bar{X}}$	Pixel variation range		$\bar{X}$	$\sigma_{\bar{X}}$	Pixel variation range	
			$\bar{X}-\sigma_{\bar{X}}$ (min)	$\bar{X}+\sigma_{\bar{X}}$ (max)			$\bar{X}-\sigma_{\bar{X}}$ (min)	$\bar{X}+\sigma_{\bar{X}}$ (max)			$\bar{X}-\sigma_{\bar{X}}$ (min)	$\bar{X}+\sigma_{\bar{X}}$ (max)
	MPRI				VARI				MGRVI			
very slight	0.096	0.004	**0.092**	**0.100**	0.148	0.007	**0.141**	**0.155**	0.190	0.008	**0.182**	**0.198**
slight	0.078	0.004	**0.074**	**0.083**	0.122	0.007	**0.115**	**0.129**	0.156	0.009	**0.147**	**0.164**
moderate	0.059	0.004	**0.055**	**0.063**	0.092	0.006	**0.086**	**0.098**	0.117	0.008	**0.109**	**0.125**
Severe	0.053	0.004	**0.049**	**0.057**	0.084	0.006	**0.078**	**0.090**	0.106	0.007	**0.098**	**0.113**
very severe	0.040	0.004	**0.036**	**0.044**	0.063	0.007	**0.056**	**0.070**	0.079	0.008	**0.071**	**0.088**

The analysis of the data regarding the range of variation in pixel values reveals that vegetation indices exhibit varying levels of overlap among defoliation degrees. To assess the significance of differences between defoliation levels, the Fischer LSD (Least Significant Difference) test was applied.

The analysis of significant differences between defoliation degreess shows that out of the eight tested vegetation indices, only three (MPRI, VARI, MGRVI) exhibit significant differences among very slight, slight, moderate, and very severe defoliation degrees, while showing non-significant differences between moderate and severe degrees observed in the year 2020.

4.1.3.3. Assessment of defoliation produced by *Lymantria dispar* based on vegetation indices calculated in the near infrared range (NIR)

Multiple vegetation indices (RVI, NDVI, EVI, GCI, GNDVI, NDRE) were calculated from aerial images captured using a drone equipped with a near-infrared (NIR) sensor. These calculations were performed to create thematic maps that highlight areas affected by defoliation at various degrees. These vegetation indices were determined from images taken at a phenological stage after the feeding of *Lymantria dispar* caterpillars had ceased, (last decade of July) in the 2020-2021 generation, when very slight and slight defoliation degree were recorded, ranging from 0-22%, for the same area covered by the RGB imaging sensor.

For each vegetation index, the main statistical parameters (mean, standard deviation, and coefficient of variation) were calculated from the statistical series formed by the pixel values within the one hectare sample areas. Additionally, through simple regression analysis, the relationship between the observed defoliation degrees in the field and the average pixel values within the corresponding areas was determined for each individual index (table 12).

Table no. 12. Basic statistical parameters of the vegetation indices obtained in near – infrared (NIR) and the correlation between pixel values and defoliation by *Lymantria dispar* in generation 2020-2021

Vegetation indices	Mean	Std. dev.	Coeff. of variation (%)	Regression equation	Coeff. of correlation (r)	Level of significance (p)
RVI	12.738	2.188	17.179	Def. (%)=32.747-1.616*RVI	-0.724	**$6.2x10^{-6}$**
NDVI	0.845	0.024	2.778	Def. (%)=138.13-149.1*NDVI	-0.716	**$8.5x10^{-6}$**
EVI	0.529	0.037	6.963	Def. (%)=55.921-82.72*EVI	-0.624	**$2.3x10^{-4}$**
GCI	7.137	0.903	12.645	Def. (%)=39.939-3.891*GCI	-0.719	**$7.7x10^{-6}$**

GNDVI	0.776	0.022	2.842	Def. (%)=136.12-159.8*GNDVI	-0.721	$7.0x10^{-6}$
NDRE	0.225	0.020	9.037	Def. (%)=52.768-180.3*NDRE	-0.751	$1.7x10^{-6}$

There are linear relationships between the pixel values obtained from all calculated vegetation indices and the observed defoliation levels in the field, with negative correlation coefficients of moderate intensity (RVI, NDVI, EVI, GCI, GNDVI) and strong intensity (NDRE), all of which are highly significant.

To establish the ranges of pixel variation across defoliation degrees, standard errors and the range of variation relative to the mean were calculated through simple variance analysis (table 13).

Table no. 13. Range of variation of pixel values for vegetation indices obtained in near – infrared (NIR), relative to standard error

Defoliation degree	$\bar{X}$	$\sigma_{\bar{x}}$	Pixel variation range		$\bar{X}$	$\sigma_{\bar{x}}$	Pixel variation range		$\bar{X}$	$\sigma_{\bar{x}}$	Pixel variation range	
			$\bar{X}-\sigma_{\bar{x}}$ (min)	$\bar{X}+\sigma_{\bar{x}}$ (max)			$\bar{X}-\sigma_{\bar{x}}$ (min)	$\bar{X}+\sigma_{\bar{x}}$ (max)			$\bar{X}-\sigma_{\bar{x}}$ (min)	$\bar{X}+\sigma_{\bar{x}}$ (max)
	RVI				NDVI				EVI			
very slight	13.945	0.607	**13.337**	**14.552**	0.858	0.007	**0.851**	**0.864**	0.545	0.011	**0.534**	**0.555**
slight	12.039	0.462	**11.577**	**12.501**	0.838	0.005	**0.833**	**0.843**	0.520	0.008	**0.512**	**0.528**
	GCI				GNDVI				NDRE			
very slight	7.542	0.260	**7.283**	**7.802**	0.786	0.006	**0.779**	**0.792**	0.237	0.006	**0.232**	**0.243**
slight	6.903	0.198	**6.705**	**7.100**	0.770	0.005	**0.765**	**0.775**	0.218	0.004	**0.214**	**0.223**

The analysis of the data from the table regarding the range of pixel values shows that none of the vegetation indices have overlaps between defoliation degrees. To assess the significance of differences between the defoliation degrees, the Fischer LSD (Least Significant Difference) test was applied.

The analysis of significant differences between the defoliation levels reveals that among the six tested vegetation indices, only three (RVI, NDVI, NDRE) capture significant differences between very slight and slight defoliation degrees recorded in 2021.

4.1.3.4. Comparative analysis of the results of defoliation assessments established on field, with those obtained based on the images captured by the drone

For the comparative analysis of field-based and aerial drone-based evaluations, it was deemed appropriate to calculate the affected areas by defoliation. To achieve this, thematic maps were created depicting the results of defoliation assessments obtained from field observations during the two years (2020 and 2021) of *Lymantria dispar* defoliator attacks (figure 12).

Figure 12. Thematic maps obtained based on ground assessments of defoliation in 2020 and 2021

Furthermore, thematic maps were also generated based on pixel value ranges specific to each defoliation degree. These ranges were determined using vegetation indices calculated in section 4.1.3.1, which were statistically proven to be significant (MPRI, MGRVI). These thematic maps enabled the

calculation of affected areas based on the established defoliation degrees in relation to the pixel value intervals (figure 13 a, b).

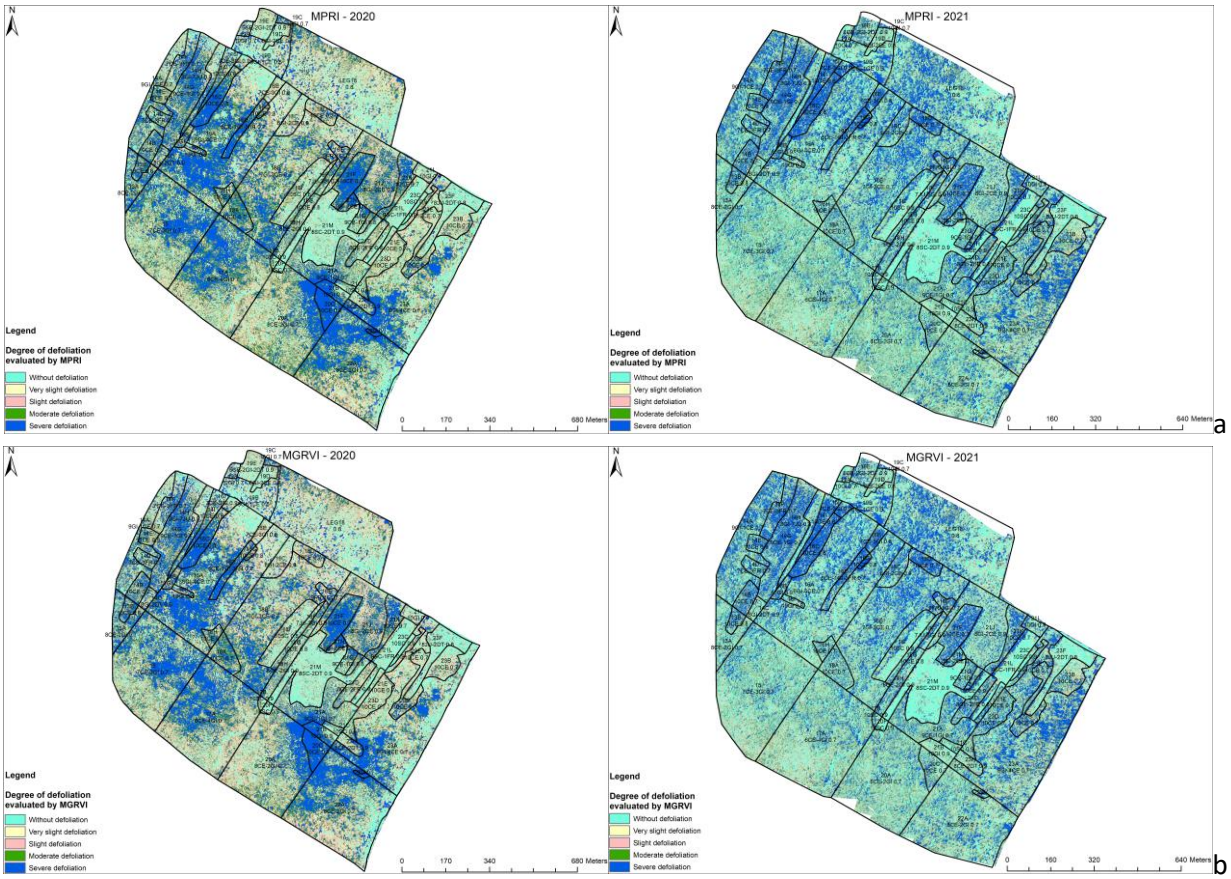

Figure 13. Thematic maps obtained based on MPRI (a) and MGRVI (b) vegetation indices for the years 2020 and 2021

The visual comparison of the two types of thematic maps (field-based - figure 12 and aerial images captured by drone - figure 13 a, b) reveals that the two statistically significant indices express trends of defoliation distribution in space that closely align with the field-based assess results for both years.

The comparative analysis of the areas by defoliation degrees calculated from the thematic maps created based on pixel value ranges for the two vegetation indices and those calculated from the thematic maps obtained through field-based assess indicated differences between the field-estimated defoliation areas and the areas calculated using these indices (figure 14).

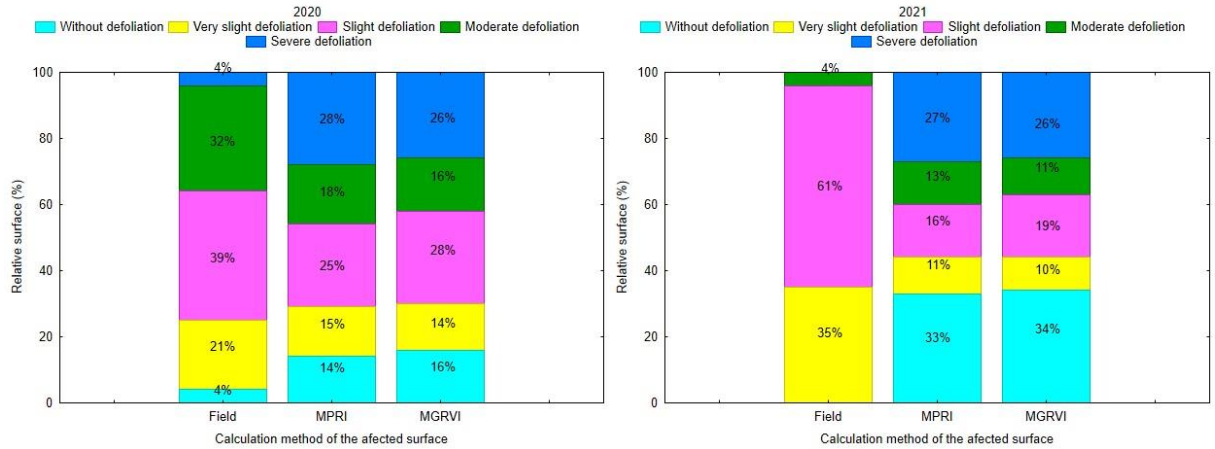

Figure 14. The comparative variation of the relative surfaces, by degrees of defoliation, calculated, on the thematic maps, obtained according to the data recorded from the ground and those obtained based on the vegetation indices (Field, MPRI, MGRVI)

The areas considered to be without defoliation and those with very slight defoliation were notably similar across all calculation scenarios in both years (25-30% in 2020 and 35-45% in 2021). These differences can be attributed to the inclusion of tree stands containing species that are not hosts for *Lymantria dispar* (such as acacia, ash, etc), which were categorized as without defoliation, and where sampling circles were not established.

The areas with moderate and severe defoliation assessed in 2020, based on the two vegetation indices and those assessed in the field, were relatively close (36-46%). There was an overestimation of moderate defoliation at the expense of severe defoliation, likely due to inherent systematic errors in field-based assessments. In 2021, with generally lower levels of defoliation, differences emerged between the field assessments and those calculated using vegetation indices. These differences can be explained by the subjectivity of field operators, who tend to classify defoliation percentages near the boundary between severity levels, and the presence of systematic underestimation errors for higher levels of defoliation due to limited visibility of the upper crown parts. Furthermore, the appearance of larger areas with severe defoliation in the case of assessments based on vegetation indices in both years can be attributed to the fact that aerial images captured by drones, with their high resolution, effectively capture gaps in the tree canopy, erroneously categorizing them as severe defoliation.

Both visual and integrated analyses of the delineated areas on the two types of thematic maps indicate that the two indices capture quite well both the areas without defoliation and those falling into various degrees of damage caused by *Lymantria dispar*.

Additionally, for the year 2021, when a drone equipped with a multispectral sensor was flown, thematic maps were created based on intervals of pixel values specific to each degree of defoliation. These maps were obtained using vegetation indices derived from the near-infrared (NIR) band, as calculated in section 4.1.3.3. and statistically proven to be significant (RVI, NDVI, NDRE).

These thematic maps have allowed for the calculation of areas based on the established degrees of defoliation in relation to the ranges of pixel variations (figure 15).

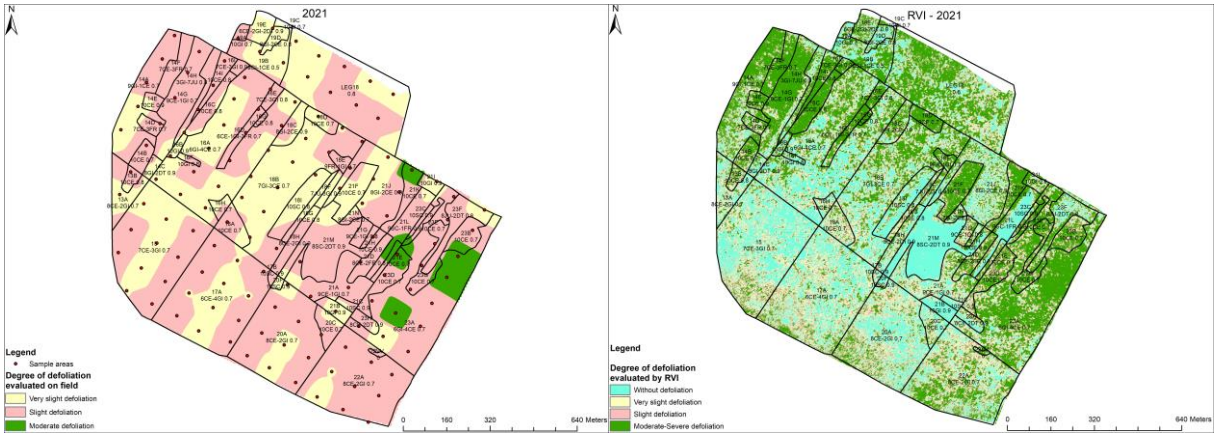

a b

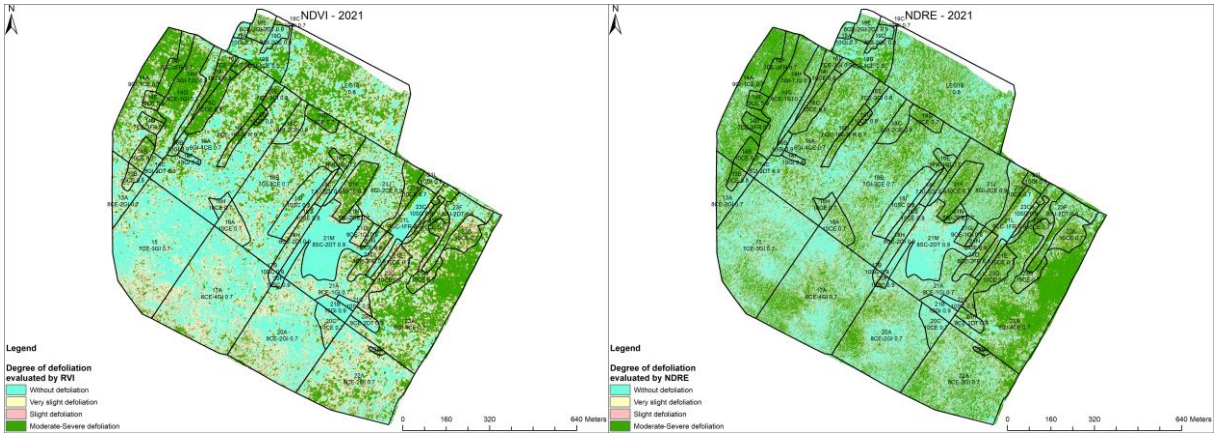

c d

Figure 15. Thematic maps obtained based on ground assessments (a) and vegetation indices RVI (b), NDVI (c) and NDRE (d) for the year 2021

The visual comparison of the two types of thematic maps (field-based - figure 15a and aerial images captured by drone - figure 15b,c,d) reveals that the three statistically significant indices demonstrate spatial distribution trends of defoliation degrees that closely resemble the results obtained from field evaluations, for both years.

The comparative analysis of the areas delineated based on the thematic maps created using the pixel value ranges for the three vegetation indices and the areas delineated on the thematic map obtained from field assess showed differences between the estimated field-based defoliation areas and the areas calculated based on these indices (figure 16).

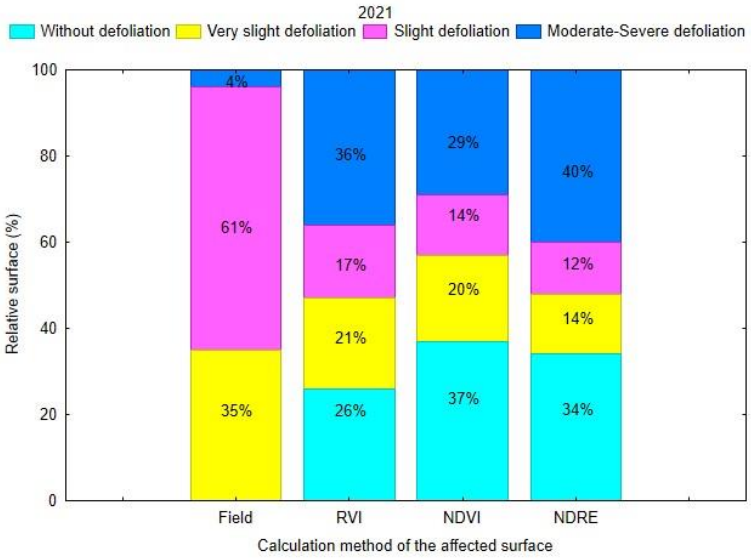

Figure 16. The comparative variation of the relative surfaces, by degrees of defoliation, calculated, on the thematic maps, obtained according to the data recorded from the field and those obtained based on the vegetation indices (Field, RVI, NDVI, NDRE)

There are significant differences between the areas considered to be without defoliation across the different calculation scenarios, ranging from 0% recorded on the field to 37% calculated using the NDVI vegetation index. The larger proportion of areas considered without defoliation, calculated through vegetation indices, can be attributed to the inclusion of tree compositions that feature species not affected by *Lymantria dispar* (e.g., acacia, ash), where sample circles were not placed. Additionally, this is influenced by the tendency of field operators to slightly overestimate defoliation at the lower threshold of the "very slight" category. When combined, the cumulative areas delineated for the two

categories (without defoliation and very slight defoliation) show relatively minor variation, ranging from 35% for field assess to 57% for assess based on the NDVI vegetation index.

Significant differences exist between the areas with moderate to severe defoliation as evaluated on the field and those identified based on vegetation indices. These differences can be largely attributed to the relatively erroneous categorization of defoliation at the boundaries of damage categories by field operators, as well as the presence of systematic underestimation errors for higher intensity defoliation due to reduced visibility of the upper parts of the crowns. Additionally, in aerial images captured by the drone, which better capture canopy gaps, there is a tendency to overestimate the areas identified with damage in the higher defoliation categories (beyond moderate).

The visual and integrated analysis of the affected areas delimited on the two types of thematic maps reveals that the three vegetation indices perform reasonably well in capturing areas without defoliation or with slight defoliation, but exhibit a tendency to overestimate the areas with higher degrees of defoliation. However, among the three vegetation indices, the NDVI index stands out for its tendency to moderate the overestimation of areas with defoliation beyond the moderate level. This is likely due to the NDVI's ability to distinguish between green vegetation and the bright background of soil reflection, expressed as the ratio between the difference of near-infrared and red spectral bands and their sum.

4.2. Monitoring and assessment of damage (discoloration) produced by *Corythucha arcuata*

4.2.1. Characteristics of damages produced by *Corythucha arcuata*

Corythucha arcuata is a species native to North America (southern Canada and several states in the USA). In Romania, it was first observed in 2015 in Arad, followed by findings in Timiș (Deta) and Bucharest (Rădac et al., 2017). In 2016, the species was identified both around Bucharest (Tomescu et al., 2018; Chireceanu et al., 2017) and in Prahova (Tomescu et al., 2018). In the Romanian conditions, *Corythucha arcuata* undergoes three incomplete generations per year and overwinters as adults in sheltered locations (Bălăcenoiu, 2022).

In cases of strong infestations, this pest can lead to premature discoloration of the tree foliage or increase the host's susceptibility to various diseases or pests. Infested trees, when viewed from a distance, display differentiated foliage coloration depending on the intensity of the attack. The discoloration of the attacked foliage progresses gradually over time, depending on the pest population density and the number of generations that have acted. The more intense the discoloration, the higher the population density of the bug and consequently, the greater the damage. Trees that are not host plants for the bug maintain their natural foliage color.

In the Ciuturica forest stand, *Corythucha arcuata* was first observed during the vegetation season of 2019, when the infestations were very slight and scattered at the forest edge or in larger gaps within the forest. In the following years, the infestations increased both in intensity and spatial distribution. By the year 2021, they had expanded to cover the entire forest stand, reaching moderate to even strong levels in certain areas.

Based on the data collected regarding the intensity of discoloration in the year 2021, recorded within the rectangular grid of sample circles, a thematic map depicting the spatial distribution of damages according to the degree of discoloration was created (figure 17).

Figure 17. Thematic map with the spatial distribution of discolorations produced by *Corythucha arcuata*, by degrees of intensity, for the 2021 generation in the Ciuturica forest stand

4.2.2. Assessment of discolorations produced by Corythucha arcuata based on Sentinel 2 satellite images

The Sentinel-2 satellite images acquired for the year 2021 on July 27, when the foliage of trees was affected by the cumulative action of adults from the third generation (hibernating), nymphs and adults from the first generation, and nymphs from the second generation, served as the basis for determining biophysical indices (LAI, FAPAR, FVC, CAB, CWC) as well as various vegetation indices calculated in the near-infrared (NIR) domain (NDVI, SAVI, MSAVI, DVI, RVI, PVI, IPVI, WDVI, TNDVI, GNDVI, ARVI, NDI45, MCARI, IRECI, PSSRa, NDRE, NRVI, IRVI, GVI, VREI) or based on the red, green, blue (RGB) bands (MPRI, VARI, GPI, ExG, GLI, RGBVI, TGI, MGRVI).

Based on each obtained biophysical and vegetation index, the main statistical parameters (mean, standard deviation, coefficient of variation) of the statistical series constituted by the specific pixel values of each sample area were determined, along with the correlation between the discolorations realized and assessed in the field and the average pixel value within the studied areas.

Through the analysis of the statistical data, the following observations were made:

- for the majority of biophysical indices (LAI, FAPAR, FVC, CAB), the correlation coefficients between the average pixel values and the average intensity of discolorations assessed on the field indicate the absence of significant relationships, except for the CWC index, where a weak correlation is present (r=-0.228, p=0.058).

- for all vegetation indices calculated in the near-infrared (NIR) domain, the correlation coefficients between the average pixel values and the average intensity of discolorations evaluated on the field are very low (insignificant), suggesting a lack of relationships between the average pixel values and the average intensity of discolorations evaluated on the field.

- for the majority of vegetation indices calculated in the visible (RGB) domain, the correlation coefficients between the average pixel values and the average intensity of discolorations evaluated on the field indicate weak relationships (r<0.5), except for the TGI index, where no significant correlation is observed (r=-0.171).

The lack of stronger relationships between the average pixel values and the average intensity of discolorations evaluated on the field for all tested indices can be explained by the relatively low resolutions of Sentinel 2 satellite images (100 m^2/pixel) and the relatively uniform distribution of

discolorations within the forest area. This uniform distribution may not allow for the differentiation of damage intensities based on the biophysical and vegetation indices derived from satellite images.

4.2.3. Assessment of discolorations produced by *Corythucha arcuata* based on drone images

4.2.3.1. Assessment of discolorations produced by *Corythucha arcuata* based on vegetation indices calculated in the visible range (RGB)

In order to create thematic maps highlighting areas affected by discoloration in various degrees of damage, several vegetation indices (MPRI, VARI, GPI, ExG, GLI, RGBVI, TGI, MGRVI) were calculated based on aerial images captured using a drone in the visible domain (RGB).

For each vegetation index, the main statistical parameters (mean, standard deviation, and coefficient of variation) of the statistical series formed by pixel values from one hectare sample areas were calculated. Additionally, through simple regression analysis, the correlation between the discoloration degrees assessed in the field and the average pixel value within the respective areas was established for each index (table 14).

Table no. 14. Basic statistical parameters of the vegetation indices obtained in visible range (RGB) and the correlation between pixel values and discoloration by *Corythucha arcuata* in generation 2020-2021

Vegetation indices	RGB indices					
	Mean	Std. dev.	Coeff. of variation (%)	Regression equation	Coeff. of correlation (r)	Level of significance (p)
MPRI	0.108	0.023	21.363	Dec. (%)=41.45-165*MPRI	-0.738	**$3.3x10^{-6}$**
VARI	0.209	0.051	24.530	Dec. (%)=39.525-75.88*VARI	-0.756	**$1.4x10^{-6}$**
GPI	0.386	0.006	1.550	Dec. (%)=152.53-334*GPI	-0.388	$3.4x10^{-2}$
ExG	32.885	3.477	10.574	Dec. (%)=6.405-52.49*ExG	0.355	$5.5x10^{-2}$
GLI	0.113	0.012	10.901	Dec. (%)=42.166-163.6*GLI	-0.392	$3.2x10^{-2}$
RGBVI	0.228	0.024	10.326	Dec. (%)=43.436-86.76*RGBVI	-0.397	$3x10^{-2}$
TGI	29.188	2.537	8.691	Dec. (%)=41.603-0.615*TGI	-0.303	$1x10^{-1}$
MGRVI	0.210	0.043	20.663	Dec. (%)=42.061-87.68*MGRVI	-0.738	**$3.2x10^{-6}$**

There are linear correlations between the pixel values obtained for all calculated vegetation indices and the discoloration degrees estimated in the field. These correlations have negative coefficients and are moderate to strong intensity for indices MPRI, VARI, and MGRVI. These correlations are highly significant. However, for indices GPI, GLI, RGBVI, and TGI, the correlations are weak and not significant. An exception is the vegetation index ExG, which has a positive but not significant correlation.

To establish the pixel value ranges across degrees of discoloration, standard errors and the range of pixel values, relative to the mean were calculated, through simple variance analysis (table 15).

Table no. 15. Range of variation of pixel values for vegetation indices obtained in visible domain (RGB), relative to standard error

Discoloration degree	$\bar{X}$	$\sigma_{\bar{X}}$	Pixel variation range		$\bar{X}$	$\sigma_{\bar{X}}$	Pixel variation range		$\bar{X}$	$\sigma_{\bar{X}}$	Pixel variation range	
			$\bar{X}$-$\sigma_{\bar{X}}$ (min)	$\bar{X}$+$\sigma_{\bar{X}}$ (max)			$\bar{X}$-$\sigma_{\bar{X}}$ (min)	$\bar{X}$+$\sigma_{\bar{X}}$ (max)			$\bar{X}$-$\sigma_{\bar{X}}$ (min)	$\bar{X}$+$\sigma_{\bar{X}}$ (max)
	MPRI				VARI				GPI			
slight discoloration	0.118	0.005	**0.113**	**0.122**	0.231	0.010	**0.221**	**0.242**	0.388	0.001	**0.386**	**0.389**
moderate discoloration	0.093	0.006	**0.087**	**0.099**	0.176	0.013	**0.163**	**0.188**	0.383	0.002	**0.382**	**0.385**
	ExG				GLI				RGBVI			
slight discoloration	32.223	0.810	31.412	33.033	0.117	0.003	**0.114**	**0.119**	0.235	0.005	**0.229**	**0.240**
moderate discoloration	33.879	0.992	32.887	34.872	0.108	0.003	**0.105**	**0.111**	0.218	0.007	**0.212**	**0.224**
	TGI				MGRVI							
slight discoloration	29.577	0.597	28.980	30.174	0.229	0.009	**0.220**	**0.238**				
moderate discoloration	28.605	0.732	27.873	29.336	0.181	0.011	**0.171**	**0.192**				

The analysis of data regarding the range of pixel values indicates that vegetation indices exhibit varying levels of overlap between different levels of discoloration. To test the significance of differences between discoloration degrees, the Fischer LSD (Least Significant Difference) test was applied.

The analysis of significance differences between degrees of discoloration, indicates that among the eight tested vegetation indices, only three (MPRI, VARI, MGRVI) capture significant differences between the slight and moderate discolorations recorded in the year 2021.

4.2.3.2. Assessment of discolorations produced by Corythucha arcuata based on vegetation indices calculated in the near infrared range (NIR)

For the aerial images captured using a drone in the near-infrared domain (NIR), a set of vegetation indices (RVI, NDVI, EVI, GCI, GNDVI, NDRE) were calculated to create thematic maps that highlight areas affected by discoloration at various degrees.

For each vegetation index, the main statistical parameters (mean, standard deviation, coefficient of variation) were computed from the statistical series formed by the values of pixels within the one hectare sample areas. Through a simple regression analysis, the correlation between the discolorations observed in the field and the average pixel values within the corresponding areas, was determined for each individual index (table 16).

Table no. 16. Basic statistical parameters of the vegetation indices obtained in near - infrared range (NIR) and the correlation between pixel values and discoloration by *Corythucha arcuata* in generation 2020-2021

Vegetation indices	NIR indices					
	Mean	Std. dev.	Coeff. of variation (%)	Regression equation	Coeff. of correlation (r)	Level of significance (p)
RVI	12.738	2.188	17.179	Dec. (%)=46.648-1.804*RVI	-0.767	$7.7x10^{-7}$
NDVI	0.845	0.024	2.779	Dec. (%)=170.08-173.3*NDVI	-0.790	$2.1x10^{-7}$
EVI	0.529	0.037	6.963	Dec. (%)=67.246-82.39*EVI	-0.589	$6.1x10^{-4}$
GCI	7.137	0.903	12.645	Dec. (%)=53.857-4.23*GCI	-0.742	$2.8x10^{-6}$
GNDVI	0.776	0.022	2.842	Dec. (%)=157.4-172.4*GNDVI	-0.738	$3.2x10^{-6}$
NDRE	0.225	0.020	9.037	Dec. (%)=61.441-167.7*NDRE	-0.663	$6.5x10^{-5}$

There are linear relationships between the resulting pixel values of all calculated vegetation indices and the realized discoloration levels estimated in the field. These relationships have negative correlation coefficients, with strong correlations for indices like RVI and NDVI, and moderate correlations for indices like EVI, GCI, GNDVI, and NDRE, all of which are statistically significant.

Through a simple variance analysis, the means and standard errors of the pixel values were computed to establish the pixel value ranges across different degrees of discoloration (table 17).

Table no. 17. Range of variation of pixel values for vegetation indices obtained in near - infrared domain (NIR), relative to standard error

Discoloration degree	$\bar{X}$	$\sigma_{\bar{x}}$	Pixel variation range		$\bar{X}$	$\sigma_{\bar{x}}$	Pixel variation range		$\bar{X}$	$\sigma_{\bar{x}}$	Pixel variation range	
			$\bar{X}$-$\sigma_{\bar{x}}$ (min)	$\bar{X}$+$\sigma_{\bar{x}}$ (max)			$\bar{X}$-$\sigma_{\bar{x}}$ (min)	$\bar{X}$+$\sigma_{\bar{x}}$ (max)			$\bar{X}$-$\sigma_{\bar{x}}$ (min)	$\bar{X}$+$\sigma_{\bar{x}}$ (max)
	RVI				NDVI				GCI			
slight discoloration	13.537	0.467	**13.070**	**14.005**	0.855	0.005	**0.850**	**0.860**	7.471	0.192	**7.279**	**7.663**
moderate discoloration	11.539	0.573	**10.966**	**12.111**	0.830	0.006	**0.824**	**0.836**	6.637	0.235	**6.402**	**6.872**
	GNDVI				NDRE							
slight discoloration	0.784	0.005	**0.780**	**0.789**	0.233	0.004	**0.228**	**0.237**				
moderate discoloration	0.763	0.006	**0.757**	**0.769**	0.214	0.005	**0.209**	**0.220**				

The analysis of the data from table 17 regarding the range of pixel values indicates that all vegetation indices, except EVI, do not exhibit overlaps between different degrees of discoloration. To assess the significance of differences between the degrees of discoloration, the Fischer LSD (Least Significant Difference) test was employed.

The analysis of significant differences between the degrees of discoloration, reveals that among the six tested vegetation indices, five (RVI, NDVI, GCI, GNDVI, NDRE) show statistically significant differences between the slight and moderate discolorations recorded in 2021.

4.2.3.3. Comparative analysis of the results of discolorations assessments established on field, with those obtained based on the images captured by the drone

The visual comparison of thematic maps generated based on vegetation indices calculated in the visible spectrum (RGB), using intervals of pixel value variation specific to each degree of discoloration, alongside the thematic map of field-assessed discolorations, reveals that among the three vegetation indices (MPRI, VARI, MGRVI), there are no apparent differences. However, for all vegetation indices, there is an observable tendency to overestimate the spatial distribution of higher degrees of damage (figure 18).

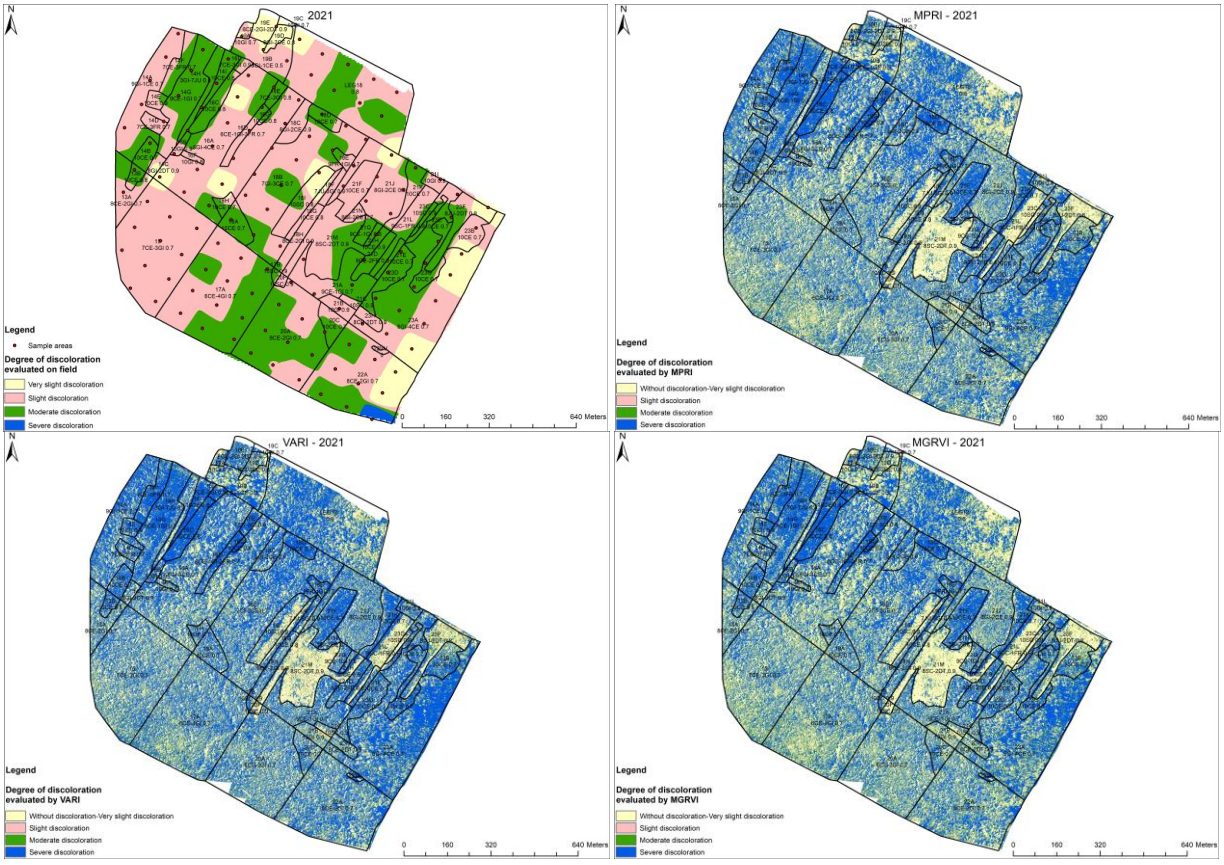

Figure 18. Thematic maps obtained based on ground assessments and vegetation indices MPRI, VARI and MGRVI for the year 2021

The same type of comparative visual analysis of thematic maps generated based on vegetation indices calculated in the near-infrared (NIR) spectrum, using intervals of pixel value variation specific to each degree of discoloration, alongside the thematic map of field-assessed discolorations, shows the same tendency of overestimating the spatial distribution of higher degrees of damage. However, this trend appears slightly less pronounced compared to that exhibited by the visible spectrum vegetation indices (figure 19).

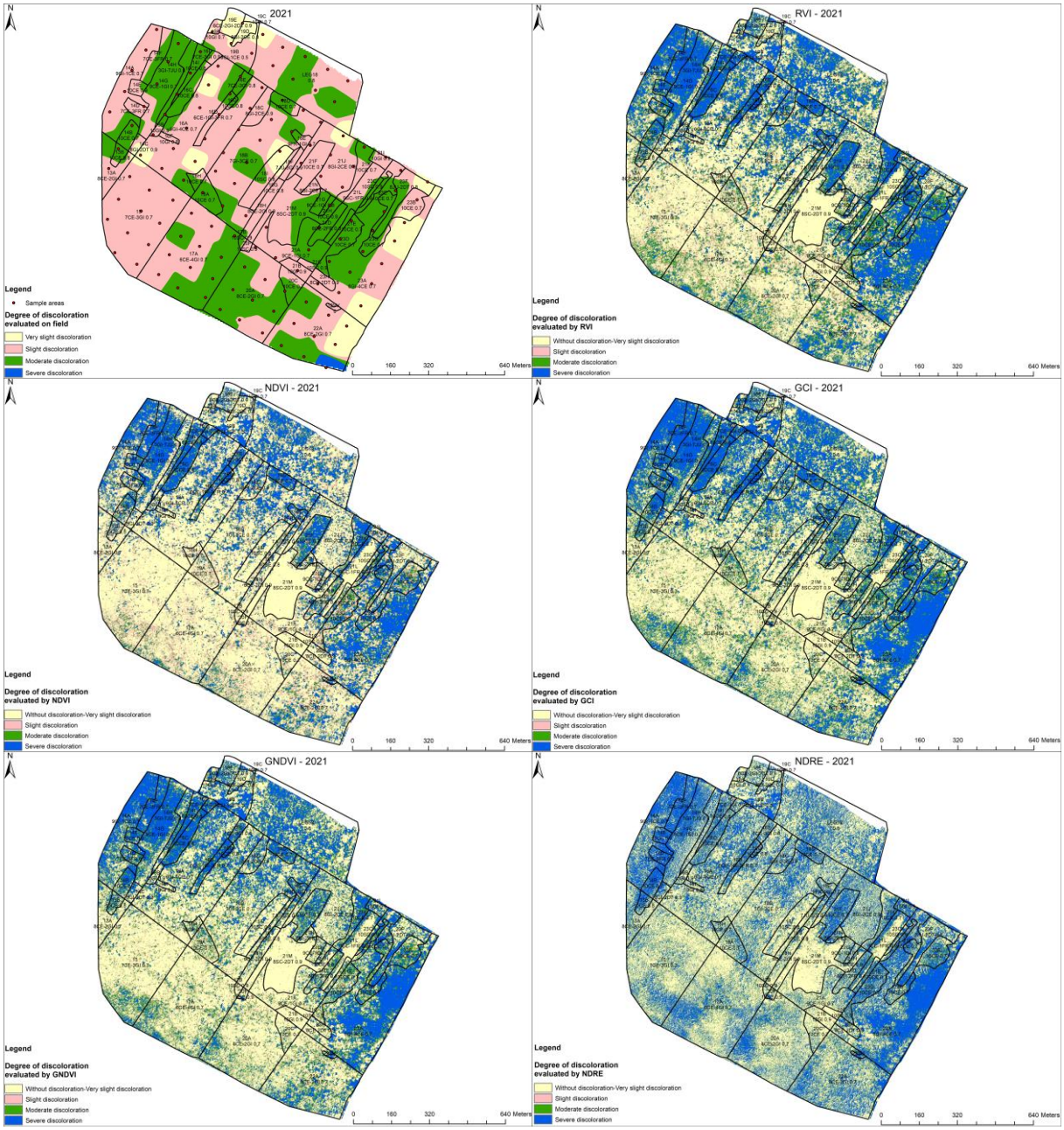

Figure 19. Thematic maps obtained on the basis of ground assessments and vegetation indices RVI, NDVI, GCI, GNDVI and NDRE for the year 2021

For a more in-depth comparative analysis, relative affected areas were calculated based on the thematic maps for different degrees of discoloration, both for indices calculated in the visible (RGB) and near-infrared (NIR) spectra, as well as for field assessments (figure 20).

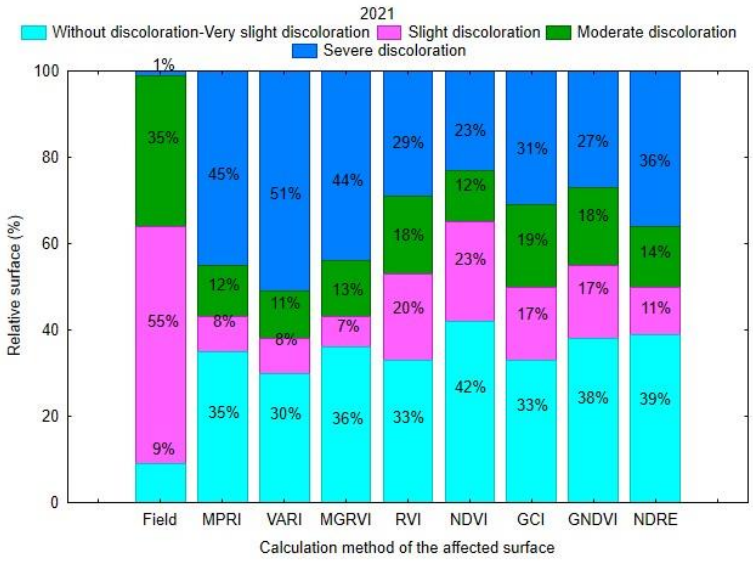

Figure 20. The comparative variation of the relative surfaces, by degrees of discoloration, calculated, on the thematic maps, obtained according to the data recorded from the field and those obtained based on the vegetation indices calculated in the visible range (MPRI, VARI, MGRVI) and near infrared (RVI , NDVI, GCI, GNDVI, NDRE)

The areas considered as "without discoloration" and "very slight discoloration" were relatively equal, delineated based on vegetation indices from the visible spectrum (30-36%) and near-infrared (33-42%). Differences between the areas assessed using vegetation indices and those assessed through field observations can be explained by the subjective nature, relatively manifested, of field operators when categorizing very slight discolorations into the slight discoloration category.

The proportions of areas evaluated with slight and moderate discolorations for vegetation indices from the RGB domain (19-20%) are lower than those obtained for vegetation indices from the near-infrared (NIR) domain (25-38%), but they are underestimated compared to the areas assessed based on field observations.

The areas with strong discolorations evaluated based on vegetation indices calculated in the visible domain (44-51%) are larger compared to those evaluated for vegetation indices determined in the near-infrared domain (23-36%). There are significant differences between the areas evaluated using both RGB-based vegetation indices and near-infrared-based vegetation indices and those assessed through field observations (1%). These substantial differences can be explained by systematic errors in underestimating higher intensity discolorations, due to reduced visibility of the upper parts of the tree canopies, and by the fact that aerial images captured by the drone have a high resolution, capturing gaps in the vegetation well and inaccurately classifying them into higher discoloration categories.

Among all the vegetation indices calculated, both in the visible (RGB) and near-infrared (NIR) domains, the Normalized Difference Vegetation Index (NDVI) stands out. It has a correlation coefficient of r=-0.790, which is highly significant ($p=2.1x10^{-7}$), and it exhibits a very strong discriminatory ability between different degrees of damage, as shown in table from chapter 4.2.3.1. NDVI shows a trend of reducing the overestimation of areas in the higher discoloration degrees. This suggests that *NDVI is the most suitable index for assessing areas affected by the type of damage caused by Corythucha arcuata's discolorations.*

5. CONCLUSIONS. ORIGINAL CONTRIBUTIONS. RESULTS DISSEMINATION

5.1. CONCLUSIONS

The results obtained through information processing and analysis during the research conducted within the doctoral thesis titled "*Monitoring and Assessment of Forest Health Using Remote Sensing Techniques*" have led to the following conclusions:

- **Regarding the quantitative and qualitative characteristics of *Lymantria dispar* and *Corythucha arcuata* populations and the damages caused by them:**
  - During the period 2018-2022, it was observed that the defoliator *Lymantria dispar* devloped an eruptive outbreak. The 2018-2019 generation went through an incipient phase, the 2019-2020 generation showed varying levels of infestations from slight to moderate to severe, distributed unevenly. The 2020-2021 generation experienced an eruption phase, while the 2021-2022 generation entered a crisis phase.
  - The sap-sucking insect *Corythucha arcuata*, first observed in the growing season of 2019, due to attacks by adults and nymphs of this insect, led to a gradual increase in leaf discoloration from very slight in the 2019 growing season to moderate and severe in the 2021 growing season.
- **Regarding the assessment of damages based on satellite imagery using biophysical and vegetation indices calculated for the visible (RGB) and near-infrared (NIR) domains:**
  - Through the conducted research, it was clearly highlighted the presence of strong and highly significant linear correlations (negative) between the pixel values of the five biophysical indices (LAI, FAPAR, FVC, CAB, CWC), determined based on Sentinel 2 satellite imagery acquired for the years 2020 and 2021, during the phenological stage of *Lymantria dispar* larval feeding cessation, and the recorded defoliation intensities on the field. Among these indices, the *Canopy Water Content* (CWC) biophysical index is considered the most suitable for assessing the defoliation caused by *Lymantria dispar*.
  - Among the pixel values of the 19 vegetation indices determined in the near-infrared (NIR) domain based on Sentinel 2 satellite imagery and the field-recorded defoliation intensities, those most suitable for evaluating defoliation caused by *Lymantria dispar* are the *Difference Vegetation Index* (DVI), *Perpendicular Vegetation Index* (PVI), and *Vogelmann Red Edge Index* (VREI). These indices exhibit a moderate correlation with the average intensity of field recorded defoliation and have overlapping ranges of pixel values for various defoliation degrees, albeit to a very limited and statistically insignificant extent.
  - Weakly significant correlations (MPRI, VARI, GPI, GLI, MGRVI) or no correlations (ExG, RGBVI, TGI) were observed between field-recorded defoliation intensities and the 8 vegetation indices determined in the visible spectrum (RGB) based on Sentinel 2 satellite imagery. All these vegetation indices exhibit overlapping ranges of pixel values for different defoliation degrees, indicating that they are not suitable for evaluating defoliation caused by *Lymantria dispar*.
  - Following the analysis of thematic maps obtained based on the pixel value ranges for the Canopy Water Content (CWC) biophysical index and the vegetation indices DVI, PVI, and VREI, identified as the most suitable for indirect evaluation of defoliation using aerial digital images, it was observed that both the CWC biophysical index and the DVI, PVI, and VREI vegetation indices tend to overestimate areas in the forest unaffected by defoliation, slightly underestimate those with very slight and slight defoliation, and overestimate surfaces affected by moderate and severe defoliation. Both visual and area-based analyses of the two types of thematic maps indicate that the *CWC biophysical index best captures both the areas unaffected by defoliation and those affected at various degrees of damage caused by Lymantria dispar*.

- Between the biophysical and vegetation indices, determined both in the near-infrared (NIR) and visible (RGB) domains based on Sentinel 2 satellite imagery, and the field-recorded intensities of discolorations, there are no significant correlations or they are very weak. This suggests that these indices cannot be used for the evaluation of damages caused by *Corythucha arcuata*.

- **Regarding the assessment of damages based on images captured with the help of drones using vegetation indices calculated in the visible (RGB) and infrared (IR) domains:**

  - Among the eight *vegetation indices* (MPRI, VARI, GPI, ExG, GLI, RGBVI, TGI, MGRVI) calculated in the visible domain (RGB) using drone-captured images, only three (MPRI, VARI, MGRVI) of them are significantly correlated. The ranges of pixel values determined for each index show larger overlaps between the very slight and slight defoliation degrees for the VARI vegetation index, and smaller overlaps for MPRI and MGRVI. This suggests their suitability for evaluating damages caused by *Lymantria dispar*.

  - Given the higher resolution provided by *drone-captured images*, among the eight vegetation indices calculated in the visible domain, only three (MPRI, VARI, MGRVI) exhibit significant differences between very slight, slight, moderate, and very severe defoliation, while showing insignificant differences between moderate and severe degrees. This confirms the ability of the *MPRI and MGRVI vegetation indices to capture differences between various degrees of damage*.

  - Between the vegetation indices (RVI, NDVI, EVI, GCI, GNDVI, NDRE) calculated in the near-infrared domain (NIR) using *drone-captured images* and the intensities of defoliation recorded from the field, there are linear relationships with negative correlation coefficients. Among them, only three (RVI, NDVI, NDRE) show significant differences between very slight and slight defoliation, *indicating the potential use of these indices for evaluating defoliation caused by Lymantria dispar.*

  - The comparative analysis of surface areas based on defoliation degrees calculated from thematic maps using the ranges of pixel variations for the two vegetation indices (MPRI and MGRVI) calculated in the visible domain (RGB), as well as those calculated from thematic maps based on field assess, highlights the areas unaffected by defoliation and those with very slight defoliation as being nearly equal. The areas affected by moderate and severe defoliation were close, with a slight overestimation of moderate defoliation compared to severe defoliation. This overestimation can be attributed to systematic errors in underestimating high-intensity defoliation as assessed from the field, due to reduced visibility of the upper parts of the tree canopies.

  - The analysis conducted for the three vegetation indices (RVI, NDVI, NDRE) calculated in the *near-infrared domain* (NIR) highlighted that all three indices capture areas without defoliation or with slight defoliation quite effectively. However, they tend to overestimate the surface areas with defoliation in the higher intensity categories. Among these three vegetation indices, NDVI stands out due to its tendency to mitigate the overestimation of areas with defoliation exceeding the moderate degree. Hence, NDVI is recommended for evaluating the defoliation caused by *Lymantria dispar.*

  - Regarding the *vegetation indices* (MPRI, VARI, GPI, ExG, GLI, RGBVI, TGI, MGRVI) calculated in the visible domain (RGB) using *drone-captured images*, significant correlations of strong intensity between pixel values and field-recorded discoloration intensities were found only for three of them (MPRI, VARI, MGRVI). Additionally, these indices exhibit significant differences between discoloration degrees, suggesting their *potential utility for evaluating damages caused by Corythucha arcuata.*

- The vegetation indices (RVI, NDVI, EVI, GCI, GNDVI, NDRE) calculated in the *near-infrared domain* (NIR) using drone-captured images exhibit highly significant correlations of strong intensity between pixel values and field-recorded decoloration intensities. Among these, only one index (EVI) doesn't show significant differences between discoloration degrees, indicating the potential use of the other five indices for evaluating damages caused by *Corythucha arcuata*. Furthermore, the analysis of surface areas, categorized by discoloration degrees, calculated on thematic maps based on pixel value ranges for both visible (RGB) and near-infrared (NIR) vegetation indices, along with those obtained from field evaluations, highlights that all significant vegetation indices tend to overestimate higher-degree discolorations, except for NDVI which displays a lesser overestimation. This makes *NDVI the most suitable for assessing discolorations caused by Corythucha arcuata.*

5.2. ORIGINAL CONTRIBUTIONS

Based on the conclusions drawn from the research conducted within the framework of this doctoral thesis, several original contributions can be formulated as follows:

- **Development for the first time of a new and modern system for monitoring and assessing the action of biotic pest agents on forests, based on satellite images and/or drone-captured imagery, equipped with multispectral sensors (RGB, NIR), complementing specific field-based activities.**
- **Approach and scientific substantiation of some methodological aspects specific to passive remote sensing, based on satellite images and/or captured by drones regarding the assessment of damage caused by defoliating and sap-sucking insects.**
- **Utilization of specialized software *ArcGIS* and *SNAP*, along with their functionalities, for monitoring and assessing the phytosanitary status of forests based on satellite and aerial digital images. These tools provide the capability to derive biophysical and vegetation indices, calculate affected areas categorized by degrees of damage, based on thematic maps.**
- **Development of a method for calculating affected areas categorized by degrees of damage, using thematic maps based on field-assessed damages. This approach enables the comparison of these maps with those obtained through remote sensing techniques, allowing for the identification of estimation errors made by field operators and systematic errors resulting from limited visibility of the upper tree canopy.**
- **Establishing the basis for determining the biophysical index derived from Sentinel 2 satellite imagery, which is considered the most suitable for assessing damages caused by defoliating insects, along with defining the range of pixel values for different degrees of defoliation.**
- **Providing the scientific rationale for determining vegetation indices calculated in the near-infrared (NIR) domain using Sentinel 2 satellite imagery, demonstrating their suitability for assessing damages caused by defoliating insects and defining the ranges of pixel values for different defoliation degrees.**
- **Testing the capacity of vegetation indices calculated in the visible domain (RGB) using Sentinel 2 satellite imagery to capture damages caused by defoliating insects.**
- **Testing the capacity of biophysical and vegetation indices calculated in both the near-infrared (NIR) and visible (RGB) domains, using Sentinel 2 satellite imagery, to capture damages caused by sap-sucking insects.**
- **Scientific establishment of vegetation indices, determined in both the near-infrared (NIR) and visible (RGB) domains using drone-captured images, considered most suitable for assessing**

damages caused by defoliating and sap-sucking insects, along with the determination of the ranges of pixel values across degrees of defoliation and discoloration.

- **Development, for the first time in our country, of an individual tree-level defoliation monitoring method through drone-captured images in the visible (RGB) spectrum. This method aims to verify and validate the suitability of selected vegetation indices for assessing damages in sample areas.**
- **Conceptualizing and implementing a method for calculating the areas affected by defoliation and discoloration, categorized by degrees of damage, based on thematic maps derived for each biophysical or vegetation index. This approach is statistically based.**

BIBLIOGRAFY

Ali, A. M., Darvishzadeh, R., Skidmore, A., Gara, T. W., O'Connor, B., Roeoesli, C., Heurich, M., Paganini, M., 2020. Comparing methods for mapping canopy chlorophyll content in a mixed mountain forest using Sentinel-2 data. International Journal of Applied Earth Observation and Geoinformation, 87, 102037.

Bălăcenoiu, F., 2022, Corythucha arcuata (Say, 1832) (Hemiptera, Tingidae) – O nouă specie de insect invazivă cu potential ridicat de vătămare în pădurile de stejar din România și Europa, Editura Silvică, Voluntari, 106 p.

Beaubien, J. and Jobin, L. 1974. ERTS-1 imagery for broad mapping of forest damage and cover types of Anticosti Island. Canadian Surveyor, 28: 164–166.

Bendig J., Yu K., Aasen H., Bolten A., Bennertz S., Broscheit J., Gnyp M. L., Bareth G., 2015, Combining UAV-based plant height from crop surface models, visible, and near infrared vegetation indices for biomass monitoring in barley, International Journal of Applied Earth Observation and Geoinformation, Vol. 39, pp 79–87.

Berryman, A.A., 1986, Forest Insects: Principles and Practice of Population Management, Plenum Press

Blackburn G. A., 1998, Quantifying Chlorophylls and Caroteniods at Leaf and Canopy Scales: An Evaluation of Some Hyperspectral Approaches, Remote Sensing of Environment, Vol. 66, Issue 3, pp 273-285

Buzatu, A., 2020, Analiza comparativă a informațiilor privind principalii agenți vătămatori, oferite de imaginile obținute cu ajutorul dronelor și a celor observate la sol, inclusiv evaluarea daunelor produse de aceștia, Raport de cercetare, Universitatea "Transilvania" din Brașov, Școala Doctorală Interdisciplinară, Facultatea de Silvicultură și Exploatări Forestiere

Cernicharo, J., Verger, A., Camacho, F., 2013. Empirical and Physical Estimation of Canopy Water Content from CHRIS/PROBA Data, Remote Sensing, Vol. 5, pp 5265-5284

Chireceanu, C., Teodoru, A., Chiriloaie, A., 2017a. First record of oak lace bug Corythucha arcuata (Tingidae: Heteroptera) in Romania. In: Trichkova T., Tomov R., Vladimirov V., Kalcheva H., Vanev Y., Uludağ A., Tyufekchiev V. (eds.), Book of Abstracts, 7th ESENIAS Workshop with Scientifi c Conference 'Networking and Regional Cooperation Towards Invasive Alien Species Prevention and Management in Europe', 28–30 March 2017, IBER-BAS, ESENIAS, Sofi a, Bulgaria, p. 97.

Ciesla W., Billings, R., Compton, J., Frament, W., Mech, R., Roberts, M., 2008. Aerial sigantures of forest damage in the Eastern United States. The Forest Health Technology Enterprise Team (FHTET). USA. 121 pp.

Clevers, J. G. P. W., 1991, Application of the WDVI in estimating LAI at the generative stage of barley, ISPRS Journal of Photogrammetry and Remote Sensing, 46 (1991), 37-47

Crippen, R. E., 1990, Calculating the Vegetation Index Faster, Remote Sensing of Environment, Volume 34, Issue 1, October 1990, Pages 71-73.

Delegido J., Verrelst J., Alonso L., Moreno J., 2011b. Evaluation of Sentinel-2 rededge bands for empirical estimation of green LAI and chlorophyll content, Sensors, Vol. 11, pp 7063–7081.

Frampton W. J., Dash J., Watmough G., Milton E. J., 2013, Evaluating the capabilities of Sentinel-2 for quantitative estimation of biophysical variables in vegetation, ISPRS Journal of Photogrammetry and Remote Sensing, Vol. 82, pp 83–92

Gitelson A. A., Merzlyak M. N., 1994, Quantitative estimation of chlorophyll-a using reflectance spectra: Experiments with autumn chestnut and maple leaves, Journal of photochemistry and photobiology. B, Biology, Vol. 22, pp 247-252

Gitelson A. A., Kaufman Y. J., Merzlyak M. N., 1996, Use of a green channel in remote sensing of global vegetation from EOS-MODIS, Remote Sensing of Environment, Volume 58, Issue 3, December 1996, Pages 289-298

Gitelson A. A., Kaufman Y. J., Stark R., Rundquist D., 2002, Novel Algorithms for Remote Estimation of Vegetation Fraction, Remote Sensing of the Environment, Vol. 80, pp 76–87.

Hall, R. J., Castilla, G., White, J.C., Cooke, B.J., Skakun, R.S., 2016, Remote sensing of forest pest damage: a review and lessons learned from a Canadian perspective, The Canadian Entomologist, Volume 148, Supplement S1: Forest Entomology in Canada: Celebrating a Century of Science Excellence, August 2016 , pp. S296 - S356

Huete, A. R., 1988, A soil-adjusted vegetation index (SAVI), Remote Sensing of Environment, Volume 25, Issue 3, August 1988, Pages 295-309

Hunt E. R. Jr., Daughtry C. S. T., Eitel J. U. H., Long D. S., 2011, Remote Sensing Leaf Chlorophyll Content Using a Visible Band Index, Agronomy Journal, Vol. 103, Issue 4, pp 1090-1099.

Junior C. K., Guimarães A. M., Caires E. F., 2016, Use of active canopy sensors to discriminate wheat response to nitrogen fertilization under no-tillage, Journal of the Brazilian Association of Agricultural Engineering, .Vol. 36, No. 5, pp 886-894

Kaufman Y. J., Tanre D., 1992, Atmospherically Resistant Vegetation Index (ARVI) for EOS-MODIS, IEEE Transactions on Geoscience and Remote Sensing, Vol. 30, No. 2, pp 261-270

Lehmann, J. R. K., Nieberding, F., Prinz, T., Knoth, C., 2015, Analysis of Unmanned Aerial System-Based CIR Images in Forestry—A New Perspective to Monitor Pest Infestation Levels, Forests, 6, 594-612; doi:10.3390/f6030594

Louhaichi M., Borman M. M., Johnson D. E., 2001, Spatially Located Platform and Aerial Photography for Documentation of Grazing Impacts on Wheat, Geocarto International, Vol. 16(1), pp 65–70.

Näsi, R., Eija Honkavaara, E., Lyytikäinen-Saarenmaa, P., Blomqvist, M., Litkey, P., Hakala, T., Viljanen, N., Kantola, T., Tanhuanpää, T., Holopainen, M., 2015, Using UAV-Based Photogrammetry and Hyperspectral Imaging for Mapping Bark Beetle Damage at Tree-Level, Remote Sensing, 7, 15467-15493; doi:10.3390/rs71115467

Qi, J., Chehbouni, A., Huete, A. R., Kerr, Y. H., Sorooshian, S., 1994, A Modified Soil Adjusted Vegetation Index, Remote Sensing of Environment, Volume 48, Issue 2, May 1994, Pages 119-126

Rădac, I. A., Pintilioaie, A. M., Manci, C. O., Rakosy, L., 2017, Prima semnalare a speciilor Amphiareus obscuriceps (Poppius, 1909) şi Corythucha arcuata (Say, 1832) în România [The first report of Amphiareus obscuriceps (Poppius, 1909) and Corythucha arcuata (Say, 1832) in Romania.]. Cel de-al XXVII-lea Simpozion Național al Societății Lepidopterologice Române, 07-08 aprilie 2017, Cluj-Napoca.

Richardson, A. J., Wiegand, C. L., 1977, Distinguishing Vegetation from Soil Background Information, Photogrammetric Engineering and Remote Sensing, Vol. 43, No. 12, December 1977, pp. 1541-1552

Richardson A., D., Jenkins J. P., Braswell B. H., Hollinger D. Y., Ollinger S. V., Smith M.-L., 2007. Use of Digital Webcam Images to Track Spring Green-Up in a Deciduous Broadleaf Forest, Oecologia, Vol. 152(2), pp 323–334.

Rouse, J.W., Haas, R.H., Schell, J.A., Deering, D.W., 1974. Monitoring Vegetation Systems in the Great Plains with ERTS. Third ERTS-1 Symposium NASA, NASA SP-351, Washington DC, 309-317.

Rullan-Silva, C. D., Olthoff, A. E., Delgado de la Mata, J. A., Pajares-Alonso, J. A., 2013. Remote monitoring of forest insect defoliation. A review, Forest Systems, 22(3): 377-391

Senseman G. M., Tweddale S. A., Anderson A. B., Bagley C. F., 1996, Correlation of Land Condition Trend Analysis (LCTA) Rangeland Cover Measures to Satellite-Imagery-Derived Vegetation Indices, US Army Corps of Engineers Construction Engineering Research Laboratories, Technical Report 97/07

Smigaj, M., Gaulton, R., Barr, S. L., Suárez J. C., 2015, UAV-borne thermal imaging for forest health monitoring: detection of disease-induced canopy temperature increase, The International Archives of the Photogrammetry, Remote Sensing and Spatial Information Sciences, Volume XL-3/W3, ISPRS Geospatial Week 2015, 28 Sep – 03 Oct 2015, La Grande Motte, France

Spurr, S.H. 1946. Aerial forest survey. In Photography by infrared. Edited by W. Clark. Wiley, New York, New York, United States of America.

Sripada, R. P., Heiniger, R. W., White, J. G., Meijer, A. D., 2006, Aerial Color Infrared Photography for Determining Early In-Season Nitrogen Requirements in Corn, Agronomy Journal, 968-977

Talerico, R.L., Walker, J.E., and Skratt, T.A. 1978. Quantifying gypsy moth defoliation. Photogrammetric Engineering and Remote Sensing, 44: 1385–1392.

Tomescu R., Olenici N., Netoiu C., Balacenoiu F., Buzatu A., 2018. Invasion of the oak lace bug *Corythucha arcuata* (Say.) in Romania: a first extended reporting. Annals. Of Forest Research, 61(2): 161-170.

Tucker, C. J., 1979, Red and Photographic Infrared Linear Combinations for Monitoring Vegetation, Remote Sensing of Environment, vol 8 (1979), pp 127-150.

Vogelmann J. E., Rock B. N., Moss D. M., 1993. Red edge spectral measurements from sugar maple leaves. International Journal of Remote Sensing, Vol. 14, No. 8, pp 1563–1575.

Vorovencii, I., 2015, Teledetecție satelitară, Editura MatrixRom, București, 600 p.

Wear, J.F. and Bongberg, J.W. 1951. The use of aerial photographs in forest insect surveys. Journal of Forestry, 49: 632–633.

Weiss, M., Baret, F., Jay, S., 2020. S2ToolBox Level 2 products LAI, FAPAR, FCOVER (Doctoral dissertation, EMMAH-CAPTE, INRAe Avignon).

Woebbecke, D. M., Meyer, G. E., Von Bargen, K., Mortensen, D. A., 1995, Color indices for weed identification under various soil, residue, and lighting conditions. Transactions of the American Society of Agricultural Engineers, 38(1), 259-269.

Yang Z., Willis P., Mueller R., 2008, Impact of band-ratio enhanced AWIFS image to crop classification accuracy, Pecora 17 – The Future of Land Imaging Going Operational, November 18 – 20, Denver, Colorado